TURUN
YLIOPISTO
UNIVERSITY
OF TURKU

DETERMINATION OF PROANTHOCYANIDIN–ANTHOCYANIN ADDUCTS IN RED WINE AND RED WINE INSPIRED HEMISYNTHESIS OF PROCYANIDIN ANALOGS

Juuso Laitila

TURUN YLIOPISTON JULKAISUJA – ANNALES UNIVERSITATIS TURKUENSIS
SARJA – SER. AI OSA – TOM. 703 | ASTRONOMICA – CHEMICA – PHYSICA – MATHEMATICA | TURKU 2023

TURUN
YLIOPISTO
UNIVERSITY
OF TURKU

DETERMINATION OF PROANTHOCYANIDIN–ANTHOCYANIN ADDUCTS IN RED WINE AND RED WINE INSPIRED HEMISYNTHESIS OF PROCYANIDIN ANALOGS

Juuso Laitila

TURUN YLIOPISTON JULKAISUJA – ANNALES UNIVERSITATIS TURKUENSIS
SARJA – SER. AI OSA – TOM. 703 | ASTRONOMICA – CHEMICA – PHYSICA – MATHEMATICA | TURKU 2023

University of Turku

Faculty of Science
Department of Chemistry
Chemistry
Doctoral programme in Exact Sciences

Supervised by

Professor, Juha-Pekka Salminen
Department of Chemistry
Natural Chemistry Research Group
University of Turku

Docent, Petri Tähtinen
Department of Chemistry
University of Turku

Docent, Maarit Karonen
Department of Chemistry
Natural Chemistry Research Group
University of Turku

Reviewed by

Dr. Véronique Cheynier
Sciences for Oenology
University of Montpellier, INRAE
Montpellier, France

Dr. Michael Jourdes
Institute of Vine and Wine Science
University of Bordeaux
Bordeaux, France

Opponent

Associate prof., Dr. Nuno Mateus
Department of Chemistry and Biochemistry
University of Porto
Porto, Portugal

The originality of this publication has been checked in accordance with the University of Turku quality assurance system using the Turnitin OriginalityCheck service.

ISBN 978-951-29-9531-8 (PRINT)
ISBN 978-951-29-9532-5 (PDF)
ISSN 0082-7002 (Print)
ISSN 2343-3175 (Online)
Painosalama, Turku, Finland 2023

UNIVERSITY OF TURKU
Faculty of Science
Department of Chemistry
Chemistry
JUUSO LAITILA: Determination of proanthocyanidin–anthocyanin adducts in red wine and red wine inspired hemisynthesis of procyanidin analogs
Doctoral Dissertation, 196 pp.
Doctoral Programme in Exact Sciences
November 2023

ABSTRACT

The chemical diversity of red wine is caused by the natural compounds that originate from grapes, and the further derivatives or adducts of the natural compounds that are formed during wine making and storage. Grapes are rich in natural pigments called anthocyanins, and in proanthocyanidins, which are the primary tannins of red wine. Both compound groups and their adducts have an impact on the valuable sensorial properties of red wine, such as colour and astringency. The oligomeric and polymeric proanthocyanidin–anthocyanin adducts pose an analytical challenge because there are several structural subgroups, and each subgroup consists of dozens of individual compounds. One consequence of this analytical challenge is that the studies about the properties and composition of proanthocyanidin–anthocyanin adducts in red wine have focused on the analysis of some individual and mainly dimeric model compounds. This might not accurately reflect the properties and functions of the compound groups as a whole.

A new analytical method based on liquid chromatography and tandem mass spectrometry was developed in this thesis for the analysis of proantocyanidin–anthocyanin adducts and other pigments in red wine. The method was utilized in the analysis of over 300 commercial red wines. The comprehensive wine set was used for studying how the composition of proanthocyanidin–anthocyanin adducts differs between wine types, how the age of the wines affects the composition of the adducts and how the oligomeric adducts contribute to the colour of red wines, for instance.

The chemical reactions occurring in red wine demonstrate how proantocyanidins and their constituting units are reactive in right conditions. This reactivity was utilized in the hemisynthesis of procyanidin analogs, which was inspired by the reactions taking place in red wine. The hypothesis was that the small structural differences in the synthetic procyanidin analogs in comparison to the natural procyanidins would have a positive effect on the important biological properties, such as interactions with proteins. Indeed, the protein precipitation capacity of procyanidin analogs was greatly improved in comparison to similar naturally occurring procyanidins, and other biological properties were affected as well.

KEYWORDS: Anthocyanin, chromatography, mass spectrometry, red wine, tannin

TURUN YLIOPISTO
Matemaattis-luonnontieteellinen tiedekunta
Kemian laitos
Kemia
JUUSO LAITILA: Proantosyanidiini–antosyaaniadduktien määrittäminen punaviinistä ja punaviinin kemian inspiroima prosyanidiinianalogien hemisynteesi
Väitöskirja, 196 s.
Eksaktien tieteiden tohtoriohjelma
Marraskuu 2023

TIIVISTELMÄ

Punaviinin kemiallinen monimuotoisuus johtuu sekä rypäleissä esiintyvistä luonnonyhdisteistä että viinien valmistuksen aikana syntyvistä luonnonyhdisteiden johdannaisista eli addukteista. Viinirypäleissä esiintyy runsaasti antosyaaneiksi kutsuttuja väriaineitä sekä proantosyanidiineja, jotka ovat punaviinin pääasiallisia tanniineja. Proantosyanidiinit ja antosyaanit vaikuttavat yhdessä moniin viinien tärkeisiin ominaisuuksiin, kuten väriin ja astringoivuuteen joko suoraan tai niiden muodostamien adduktien välityksellä. Oligo- ja polymeeriset proantosyanidiini–antosyaaniadduktit ovat kuitenkin analyyttisesti haastavia yhdisteitä, koska erilaisia rakenteellisia alaryhmiä on useita ja niistä kukin sisältää kymmenittäin erilaisia yhdisteitä. Analyyttisten haasteiden vuoksi proantosyanidiini–antosyaaniadduktien ominaisuuksia ja koostumusta viineissä on jouduttu arvioimaan aiemmin yksittäisten ja lähinnä dimeeristen malliyhdisteiden avulla, mikä ei välttämättä anna todellista kuvaa kokonaisista yhdisteryhmistä.

Tässä väitöskirjatyössä kehitettiin uusi nestekromatografiaa ja tandemmassa-spektrometriaa hyödyntävä yhdisteryhmäkohtainen analyysimenetelmä punaviinin monimuotoisten väriaineadduktien havaitsemiseksi. Kehitettyä menetelmää käytettiin yli 300 kaupallisen punaviinin analysointiin. Laajan viiniaineiston avulla selvitettiin muun muassa miten proantosyanidiini–antosyaaniadduktien koostumus vaihtelee eri viinien välillä, minkälaisia muutoksia viinin ikä saa aikaan yhdistekoostumuksessa ja mikä on oligomeeristen ja polymeeristen pigmenttien rooli punaviinien värin muodostuksessa.

Proantosyanidiinit ovat sopivissa olosuhteissa reaktiivisia yhdisteitä. Tätä reaktiivisuutta hyödynnettiin yhdessä osatyössä valmistamalla hemisynteettisesti punaviinin kemian inspiroimia prosyanidiinien kaltaisia yhdisteitä eli prosyanidiini-analogeja. Hypoteesina oli, että prosyanidiinianalogien pienet rakenteelliset erot luontaisiin prosyanidiineihin nähden vaikuttavat positiivisesti biologisesti tärkeisiin ominaisuuksiin, kuten vuorovaikutuksiin proteiinien kanssa. Proteiininsaostuskapasiteetti olikin merkittävästi parempi prosyanidiinianalogeilla kuin vastaavilla luontaisilla prosyanidiineilla ja lisäksi analogien muutkin biologiset ominaisuudet poikkesivat luontaisista prosyanidiineista.

ASIASANAT: Antosyaani, kromatografia, massaspektrometria, punaviini, tanniini

Table of Contents

Abbreviations

A	Anthocyanin
BSA	Bovine serum albumin
CE	Collision energy
CV	Cone voltage
DAD	Diode array detector
DBA	Dihydroxybenzaldehyde
EGCG	Epigallocatechin-3-*O*-gallate
ESI	Electrospray ionization
FL	Flavan-3-ol monomer
HESI	Heated electrospray ionization
HPLC	High-performance liquid chromatograpy
HRMS	High-resolution mass spectrometry
LOA	Large oligomeric adduct
mDP	Mean degree of polymerization
MOA	Medium-sized oligomeric adduct
MRM	Multiple reaction monitoring
MS	Mass spectrometry
MS/MS	Tandem mass spectrometry
Mv	Malvidin glycoside
PA	Proanthocyanidin
PC	Procyanidin
PD	Prodelphinidin
PBS	Phosphate buffered saline
PLS-DA	Partials least squares discriminant analysis
PLSR	Partial least squares regression
QM	Quinone methide
RDA	Retro Diels–Alder
SOA	Small oligomeric adduct
SRM	Selected reaction monitoring
TBA	Trihydroxybenzaldehyde
UPLC	Ultra-performance liquid chromatography

List of Original Publications

This dissertation is based on the following original publications, which are referred to in the text by their Roman numerals:

I Laitila, J. E., Suvanto, J., and Salminen, J.-P. Liquid chromatography–tandem mass spectrometry reveals detailed chromatographic fingerprints of anthocyanins and anthocyanin adducts in red wine. *Food Chemistry*, 2019; 297: 138–151.

II Laitila, J. E., and Salminen, J.-P. Relevance of the concentrations and sizes of oligomeric red wine pigments to the colour intensity of commercial red wines. *Journal of Agricultural and Food Chemistry*, 2020; 68: 3576–3584.

III Laitila, J. E. Composition and evolution of oligomeric proanthocyanidin–malvidin glycoside adducts in commercial red wines. *Food Chemistry*, 2021; 340: 127905.

IV Laitila, J. E., and Salminen, J.-P. Quantitative and qualitative composition of proanthocyanidins and other polyphenols in commercial red wines and their contribution to sensorially evaluated tannicity. *Under review in Food Research International.*

V Laitila, J. E., Tähtinen, P. T., Karonen, M., and Salminen, J.-P. Red Wine Inspired Chemistry: Hemisynthesis of Procyanidin Analogs and Their Protein Precipitation Capacity, Octanol–Water Partition and Stability in Phosphate-Buffered Saline. *Accepted to Journal of Agricultural and Food Chemistry*.

1 Introduction

1.1 Diversity of natural polyphenols in red wine

Most natural products in red wine originate from grapes. These include anthocyanins, which give the colour to the skins of the grapes, and proanthocyanidins (PAs), which are the main tannins in red wine (Figure 1; Baldi et al., 1995; Hanlin et al., 2011; Mazza, 1995). These two compound groups are the most important ones for many of the sensorially valuable properties of red wine either directly or through various chemical reactions that take place during wine making (Chira et al., 2015; Escribano-Bailón et al., 2019; Freitas & Mateus, 2011; García-Estévez et al., 2018).

PAs are oligomers and polymers that consist of flavan-3-ol monomers (FL). The most common FLs in nature are catechins and gallocatechins, which are called procyanidin (PC) and prodelphinidin (PD) units, respectively, when they are incorporated in PAs (Figure 1). PAs in red wine are almost exclusively built from PC and PD units, with the former units constituting approximately 60–90% of the PAs (Gómez-Plaza et al., 2016; Gris et al., 2011; Hanlin et al., 2011). PAs are extracted from both the skins and seeds of grapes, and some of the seed PAs are galloylated leading to 1–3% of PAs being galloylated in red wine (Gris et al., 2011; Hanlin et al., 2011).

Anthocyanins are coloured flavonoids that consist of an aglycone moiety called the anthocyanidin unit, and of one or more glycosidic units. In red wine, there are three typical glycosidic units that are attached to anthocyanidins via the C3 carbon (Figure 1). The three glycosidic units are glucoside, acetylglucoside and coumaroylglucoside (Bakker & Timberlake, 1985; Mazza, 1995). Anthocyanins are unique flavonoids because they are in a pH dependent equilibrium between various forms (Figure 1; Brouillard & Delaporte, 1977; Brouillard & Dubois, 1977; Pina et al., 2015). Other factors, such as temperature, affect the equilibrium as well but pH is the single most important variable affecting equilibrium. The flavylium cation is the predominant form in very acidic environment (pH < 2) and it has a bright red colour. However, anthocyanins are mainly in colourless hemiacetal form in the typical moderately acidic conditions (pH 3–4) of red wine. Both equilibrium forms are important in the formation of anthocyanin adducts, as will be discussed later.

Further equilibrium forms exist as well as pH rises, but these are not relevant in the typical pH range of red wine. Although red wine contains anthocyanins based on five different anthocyanidins (Figure 1), the malvidin glycosides (Mv) are the most abundant anthocyanins in red wine (Mazza, 1995).

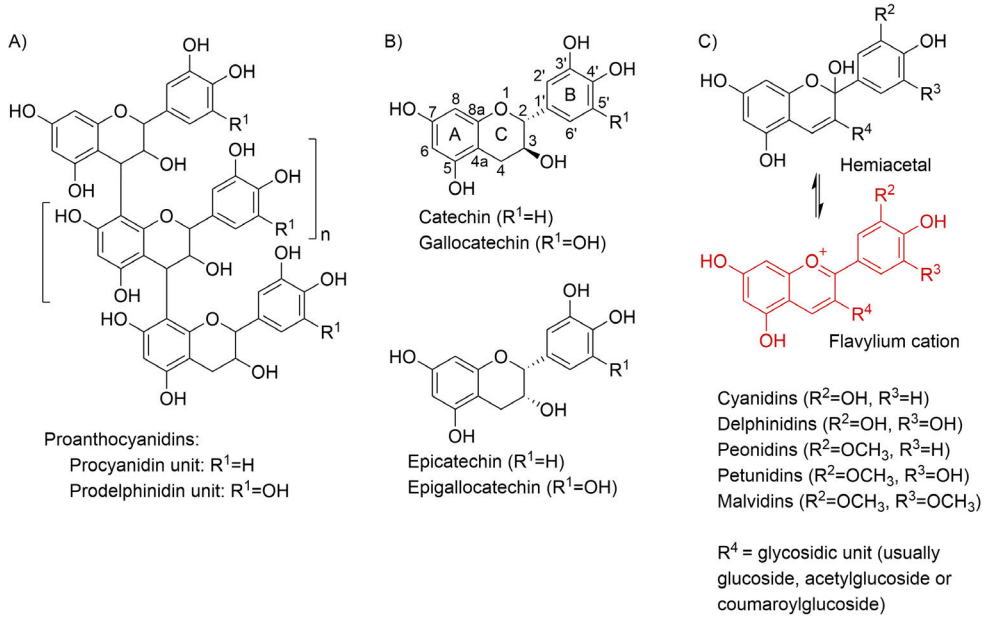

Figure 1. Structures of proanthocyanidins (A), four flavan-3-ol monomers found in red wine (B; Lukić et al., 2019) and the typical anthocyanins found in red wine (C; Mazza, 1995). The numbering and lettering of the carbon skeleton of flavonoids is presented in the structures of catechin and gallocatechin (B). The presented proanthocyanidin structure is an arbitrary example of their general structure and it omits positional isomerism and stereochemistry of the intramolecular linkages between the constituting units, and existence of A-type ether linkages, for instance. Anthocyanins (C) are presented in their coloured flavylium cation form and in their colourless hemiacetal form, which are the two most important equilibrium forms in red wine. Refer to Pina et al. (2015) for the full pH-dependent equilibrium network of anthocyanins.

Besides PAs and anthocyanins, red wines are rich in other specialized plant metabolites as well. For instance, dozens of stilbenes have been characterized from red wine ranging from simple resveratrols to more complex oligomeric stilbenes (Moss et al., 2013). Red wine contains several types of flavonols based on kaempferol, quercetin and myricetin aglycones, and their methoxylated derivatives (Castillo-Muñoz et al., 2007; Fanzone et al., 2012). Red wine also contains flavanols, mainly taxifolins, albeit their concentration is often lower than the concentrations of the flavonols (Fanzone et al., 2012; Lukić et al., 2019). Flavonols and flavanols are present both as free aglycones and as glycosides. Smaller phenolic acids, e.g., hydroxycinnamic acids and

hydroxybenzoic acids are present in red wine as well (Fanzone et al., 2012; Lukić et al., 2019). Red wine can additionally contain *C*-glycosidic ellagitannins, such as vescalagin and castalagin, if the wine is aged in oak barrels or it otherwise comes to contact with oak chips during manufacturing (García-Estévez et al., 2012).

1.2 Diversity of anthocyanin adducts in red wine

Despite the rich content of naturally occurring polyphenols, the unique complexity of red wine stems from the chemical reactions that take place during wine making and storage. The reactions leading to the formation of adducts of PAs and anthocyanins are enabled by their nucleophilic and electrophilic properties (Dangles & Fenger, 2018). Both compound groups have a similar structural moiety, which is the A-ring (Figure 1). There are three *o*/*p* activators in the A-ring that each enhance the nucleophilicity of the C6 and C8 carbons. The nucleophilic properties of anthocyanins are only displayed when anthocyanins are in their neutral hemiacetal forms, whereas the flavylium cation has two electrophilic centres, namely the C2 and C4 carbons (Figure 1C). In other words, anthocyanins possess both nucleophilic and electrophilic properties. Both properties play a role in red wine because both the flavylium cation and hemiacetal forms are present significant proportions in the mildly acidic conditions of red wine (Dangles & Fenger, 2018; Pina et al., 2015). The nucleophilic properties of anthocyanins are crucial in the formation of oligomeric PA–anthocyanin adducts, while the electrophilic properties are needed in the formation of both the PA–anthocyanin adducts and monomeric anthocyanin adducts. The adducts of anthocyanins are broadly classified as the first generation adducts, which are the primary adducts formed directly from anthocyanins, and as the second generation adducts, which are the further derivatives of the first generation adducts of anthocyanins (Freitas & Mateus, 2011).

1.2.1 Monomeric anthocyanin adducts

Pyranoanthocyanins were the first monomeric anthocyanin adducts that were accurately characterized from red wine (Figure 2; Bakker et al., 1997; Bakker & Timberlake, 1997; Cameira-dos-Santos et al., 1996; Fulcrand et al., 1996, 1998). The most elementary pyranoanthocyanins with only an additional pyran ring (D-ring; Figure 2A) are formed through an electrophilic addition reaction between anthocyanins and various aldehydes or ketones. Reactions with pyruvic acid and oxaloacetic acid lead to the formation of carboxypyranoanthocyanins, which are also known as A-type vitisins (Araújo et al., 2017; Fulcrand et al., 1998). Reactions with acetone and acetoacetic acid lead to the formation of methylpyranoanthocyanins, and the reactions with acetaldehyde lead to the formation of unsubstituted

pyranoanthocyanins, i.e., B-type vitisins (Bakker & Timberlake, 1997; Hayasaka & Asenstorfer, 2002; He et al., 2006). Carboxypyranoanthocyanins and methylpyranoanthocyanins can each be produced from two different starting materials, but pyruvic acid is thought to be the more relevant starting material for carboxypyranoanthocyanins in red wine, while oxaloacetic acid is thought to be more common in the formation of the methylpyranoanthocyanins (Araújo et al., 2017; Freitas & Mateus, 2011).

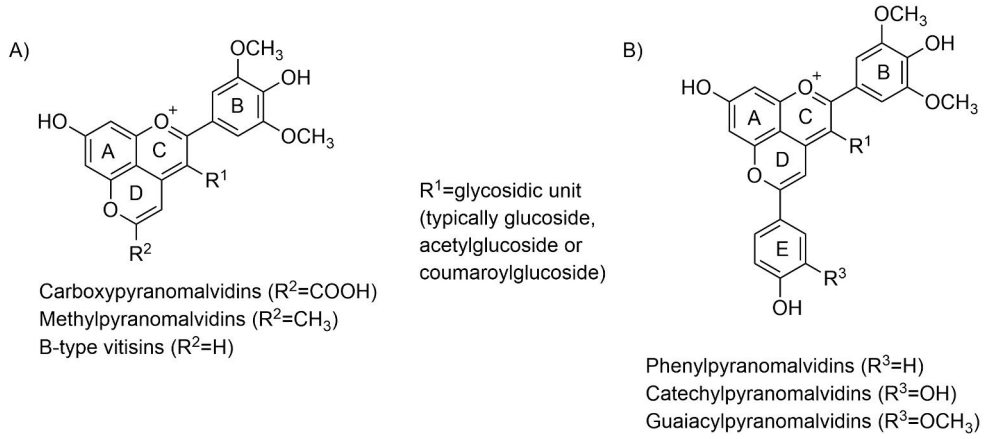

Figure 2. Structures of common pyranoanthocyanins found in red wine. The pyranoanthocyanins with a phenolic E-ring (B) are additionally known as pinotins. The pyranoanthocyanin structures are presented as adducts of malvidin glycosides because malvidin glycosides are the most abundant anthocyanins in red wine (Mazza, 1995), and the malvidin-based adducts are relevant for the experimental section of this thesis.

The very first pyranoanthocyanins that were characterized from red wine were pinotins (Figure 2B; Cameira-dos-Santos et al., 1996; Fulcrand et al., 1996). Pinotins are be formed when anthocyanins react with either vinylphenols or hydroxycinnamic acids via an electrophilic addition reaction, and structurally they possess an additional phenolic ring (E-ring) in comparison to the simplest pyranoanthocyanins (Figure 2). The reactions with *p*-coumaric acid, caffeic acid, ferulic acid and sinapic acid lead to the formation of pinotins with a phenyl, catechyl, guaiacyl and syringyl groups, respectively (Schwarz et al., 2003). These same compounds can be formed from reactions with 4-vinylphenol, 4-vinylcatechol, 4-vinylguaiacol and 4-vinylsyringol as well. However, only 4-vinylphenol and 4-vinylguaiacol have been found in wine (Lopez et al., 2002; Schwarz et al., 2003), and the enzymes of *Saccharomyces cerevisae* have been shown to only be able to decarboxylate *p*-coumaric and ferulic acids into corresponding 4-vinylphenol and 4-vinylguaiacol (Chatonnet et al., 1993).

Carboxypyranoanthocyanins can react further to yield monomeric adducts of the second generation, such as certain portisins and oxovitisins (J. He, Oliveira, et al., 2010; Mateus et al., 2006; Oliveira et al., 2007). These pigments are not relevant for the experimental section of this thesis and, therefore, they are not covered in detail.

1.2.2 Proanthocyanidin–anthocyanin adducts

The existence of polymeric pigments in red wine was initially suggested in the 1960s and 1970s (Jurd, 1969; Somers, 1971; Timberlake & Bridle, 1976). A series of experiments was performed that showed how the colour of red wines reacted to changes in pH differently than solutions of pure anthocyanins did, and that the concentrations of anthocyanins decreased as wine aged while the red colour remained (Jurd, 1969). Polymeric pigments with either direct linkages or methylmethine linkages between the PAs and anthocyanins were recognized as the unidentified compounds responsible for the colour of wines (Somers, 1971; Timberlake & Bridle, 1976). First direct measurements of dimeric adducts in red wine were achieved in the late 1990s and early 2000s thanks to the advancements in LC–MS techniques (Hayasaka & Kennedy, 2003; Salas et al., 2004; Saucier et al., 1997; Vivar-Quintana et al., 1999). Nowadays, it is recognized that even a simple model solution with few starting materials, e.g., epicatechin, malvidin glucoside and acetaldehyde readily cascades to complex mixtures of different types of oligomeric adducts of varying degree of oligomerization, and similar phenomenon is expected to take place in red wine as well (Vallverdú-Queralt et al., 2017).

There are three main types of adducts of PAs and anthocyanins (PA–A). Before the different subgroups are discussed, a small note must be made about the nomenclature. The abbreviation PA–A is used throughout to refer to adducts of PAs and anthocyanins in general, without specifying the exact structural sub-group. Corresponding nomenclature is used when discussing specifically the adducts of PAs and malvidin glycosides (PA–Mv). The structural subgroups have their own abbreviations, and some resemble closely the general notation, but they should not be confused with one another. The three main subgroups of PA–A adducts are introduced with PAs and anthocyanins, but the experimental work in this thesis, and most work done in literature, has been conducted with corresponding PA–Mv adducts. This is because PA–Mv adducts are the most abundant of the oligomeric adducts in red wines due to the malvidin glycosides being the most abundant anthocyanins.

In PA–A^+ adducts, the anthocyanin unit is the terminal unit in the oligomer or polymer (Figure 3A; Salas et al., 2003, 2004). The formation of these adducts requires that a PA must first undergo acid-catalysed depolymerization to yield carbocationic intermediate from the extension units. Depolymerization of PAs is known to take place in typical conditions of red wines (Dallas et al., 1996; Haslam,

1980). An anthocyanin then attacks the released carbocationic PA in its nucleophilic hemiacetal form to yield the PA–A^+ adduct. The nucleophilic properties of anthocyanins are required in the formation of PA–methylmethine–A^+ adducts as well (Figure 3B). The methylmethine-linked adducts are formed through two subsequent electrophilic aromatic substitution reactions between a PA, an anthocyanin and acetaldehyde (Es-Safi et al., 2002; Lee et al., 2004). FLs can participate in these reactions as well, unlike to the formation of PA–A^+ adducts.

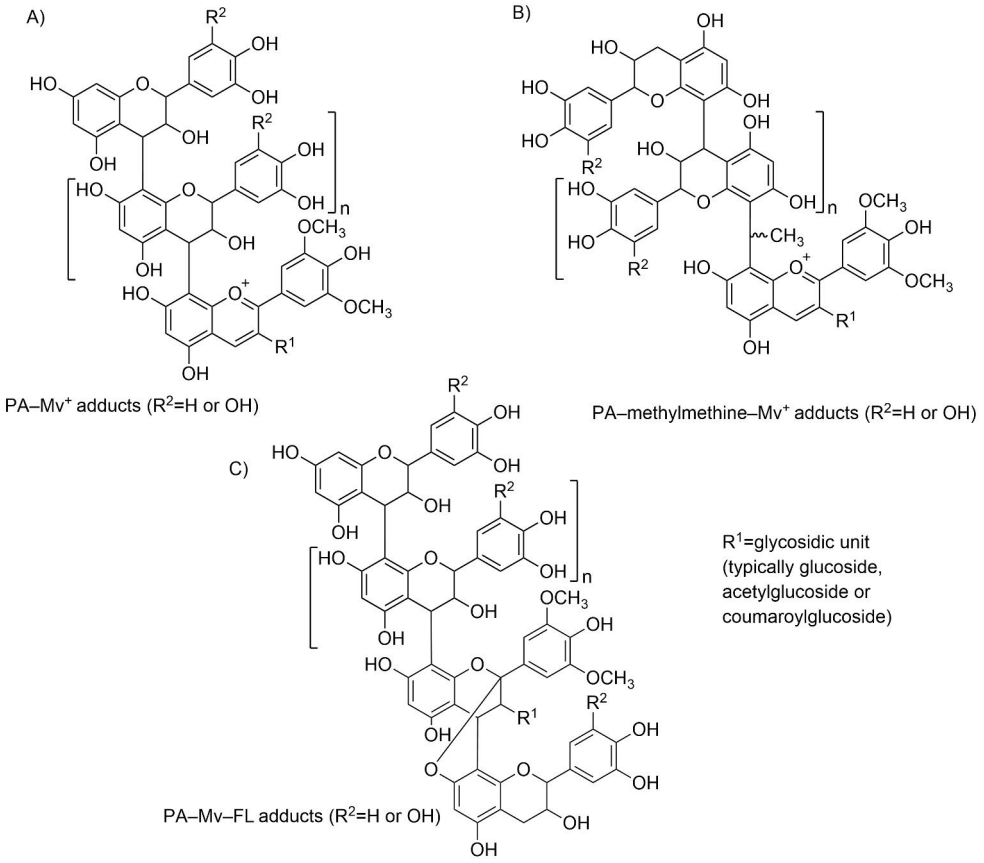

Figure 3. General structures of three different groups of oligomeric proanthocyanidin–anthocyanin adducts found in red wine. The adduct groups are presented as adducts of malvidin glycosides because malvidin glycosides are the most abundant anthocyanins in red wine (Mazza, 1995), and the malvidin-based adducts are relevant for the experimental section of the thesis. Abbreviations: PA, proanthocyanidin; Mv, malvidin glycoside; FL, flavan-3-ol monomer.

Anthocyanins can also form oligomeric adducts via their electrophilic flavylium cation form (Remy et al., 2000; Remy-Tanneau et al., 2003; Salas et al., 2003). In

this case, a PA or an FL attacks the electrophilic C4 carbon of an anthocyanin to yield a product where the anthocyanin unit is initially in a flavene form. Then, further C–O coupling leads to colourless bicyclic adduct that closely resembles A-type PAs (Salas et al., 2003). It has also been suggested that the flavene form could oxidize back to the flavylium cation form and further to xanthylium-type structures (Salas et al., 2003). If the attacking nucleophile is an FL, then the resulting A–FL dimer eventually forms a structure that is shown in Figure 3C, where the bicyclic moiety is the terminal unit (PA–A–FL). If the initial attacking nucleophile is a PA, then the bicyclic structure unit is the last extension unit (A–PA).

All above-described mechanisms are the initial mechanisms that lead to the formation of different types of PA–A adducts but each adduct group can presumably increase in chain length by participating in the constantly on-going depolymerization and repolymerization reactions of PAs. For instance, this would lead to the formation of PA–A–FL adducts (Figure 3C) from the dimeric A–FL adducts. Other types of oligomeric adducts that are formed from anthocyanins, pyranoanthocyanins, PAs and vinyl PAs have been characterized in red wine and in model solutions (Freitas & Mateus, 2011; He et al., 2012). Their direct analysis is not part of the experimental section of this thesis and, therefore, they are not introduced further here. The other oligomeric adducts have been covered in reviews by Freitas and Mateus (2011) and He et al. (2012), for instance.

1.3 Analysis of anthocyanin adducts in red wine

1.3.1 Analysis of monomeric and small oligomeric adducts

Even though there are plenty of different monomeric pigment groups in red wine, most of them can be detected and (semi)quantified straight from red wine with modern LC–MS methods without excessive pre-purification. For instance, Willemse et al. (2015) utilized two-dimensional chromatography with hydrophilic interaction and C18 reversed phase columns, and high-resolution mass spectrometry to detect 94 individual pigments in red wine. All major groups of the first generation of adducts and some of the second generation of adducts were covered, including the various types of dimeric and trimeric PA–A adducts as well. Elsewhere, Alberts et al. (2012) utilized cleverly the fact that there are typically only three different glycosidic moieties in anthocyanins in red wine, and thereby in the adducts of anthocyanins as well. Alberts et al. (2012) developed a tandem mass spectrometric method, which utilized neutral loss scans set to detect the neutral losses of the known glycosidic units. This enabled them to detect 121 pigments that, again, covered all the major monomeric pigment groups in red wines together with the main dimeric PA–A adducts (Alberts et al., 2012). Untargeted metabolomic analyzes enabled by

high-resolution mass spectrometry have also been applied in analysis of red wine, but only anthocyanins, their monomeric adducts, and dimeric PA–A adducts were reported (Arapitsas et al., 2020). However, oligomeric adducts up to nonamers have been detected in a simple model solution containing only epicatechin, malvidin glucoside and acetaldehyde by using high-resolution mass spectrometry and by using appropriate chemometric tools (Vallverdú-Queralt et al., 2017). This confirms that the basic polyphenolic components in red wine have the capability to oligomerize well beyond the dimeric and trimeric stage, at least in model solutions.

1.3.2 Challenges in analysis of higher oligomeric adducts

As mentioned in the previous chapter, the main dimeric PA–A adducts can be detected using various mass spectrometric mehods, but the higher oligomers usually remain undetected (Alberts et al., 2012; Arapitsas et al., 2020; Boido et al., 2006; Willemse et al., 2015). However, few methods exist in literature that have been utilized in the quantitative or semiquantitative detection of higher polymeric pigments in red wine. One of the most popular methods is the spectroscopic method by Harbertson et al. (2003) that combines precipitation of oligomers and polymers with bovine serum albumin (BSA) and bleaching of pigments by bisulfite to detect small polymeric pigments (SPP) and large polymeric pigments (LPP). The detection of SPPs and LPPs, however, is based on the chemical properties of the pigments rather than their structures. Therefore, it is problematic to conclusively determine what is being measured. For instance, most of the monomeric anthocyanin adducts are resistant to bleaching by bisulfite, as are the dimeric PA–methylmethine–Mv^+ adducts, while the dimeric PA–Mv^+ adducts are equally susceptible to bleaching by bisulfite as anthocyanins (Dueñas et al., 2006; J. He, Carvalho, et al., 2010; Nave et al., 2010; Quijada-Morín et al., 2010). The ability of the oligomeric adducts to precipitate proteins might also vary greatly between different adduct groups.

The detection of oligomeric pigments by the method of Harbertson et al. (2003) is universal by design, and specific subgroups of polymeric pigments cannot be detected separately. The same is true for many other methods in the literature as well. One example is the HPLC method of Peng et al. (2002) where polymeric pigments are detected as a late-eluting hump at 520 nm. Second example is the gel-permeation method of Bindon et al. (2014) where the polymeric pigments are separated by their size using size-exclusion chromatography, but they are still detected as a single broad chromatographic hump using UV-detection.

Structural specificity for oligomeric PA–Mv adducts in red wine has been achieved with a modified phloroglucinolysis method of Zeng et al. (2016). Zeng et al. (2016) characterized marker compounds produced in phloroglucinolysis for four different groups of PA–Mv adducts by high-resolution mass spectrometry. The PA–

Mv adducts presented in Figure 3 were amongst the four groups for which marker compounds were characterized. Additionally, Drinkine et al. (2007b, 2007a) characterized marker compounds for methylmethine-linked PAs that were also produced during phloroglucinolysis, which further underlines the applicability of phloroglucinolysis in analysis PA adducts in red wine. Phloroglucinolysis will be returned to in chapter 1.5., where a brief description of its principle is given.

1.4 Properties of proanthocyanidin–anthocyanin adducts

Most of the understanding about the basic properties of the PA–A adducts in red wine comes from studies that focused on the analysis of individual dimers of trimers, which is partly connected to the previously described analytical challenges. For instance, the evolution of various types of dimeric PA–Mv adducts in red wine is well documented in the literature (Alcalde-Eon et al., 2006; Arapitsas et al., 2012; Blanco-Vega et al., 2014; Boido et al., 2006). The results obtained with the dimers have been extended to concern the compound groups, as no direct evidence about their evolution has been obtained at the compound group level. Another basic function of oligomeric and monomeric pigments, i.e., their impact on colour, has also been established by studying properties of individual dimers (Cruz et al., 2010; Dueñas et al., 2006; Nave et al., 2010). Fascinating differences in various properties have been discovered between different types of dimeric PA–Mv adducts, and it is certainly important to understand the effects that the structural differences cause in the sensorially valuable properties of the dimers. For example, the thermodynamic and kinetic properties of the malvidin glucoside unit in a dimeric FL–Mv^+ adduct were unchanged when compared to free malvidin glucoside (Nave et al., 2010). On the other hand, the structural equilibrium network of the malvidin glucoside unit in dimeric FL–methylmethine–Mv^+ adducts was greatly affected as the proportion of the colourless hemiacetal form was reduced, or it did not occur at all, in favour of the quinoidal base form (Dueñas et al., 2006).

While it is possible that the smallest oligomers could reflect the behaviour and properties of higher oligomers, it is not given that this is the case. For instance, differences in chromatic properties were observed between a dimer and a trimer consisting of a pyranomalvidin glucoside and catechin units, i.e., chromatic properties were affected by the degree of oligomerization (He, Carvalho, et al., 2010). The wavelength of the maximal absorption of the flavylium cation form of the trimer was 8 nm higher than the absorption maximum of the dimer. Additionally, molar absorptivities of the two oligomers reacted differently to changes in pH and the authors concluded that the colourless FL moieties had impact on the colour expression of the chromophore by co-pigmentation (He, Carvalho, et al., 2010).

Finally, if the evolution and other properties of polymeric pigments are studied using more universal methods that detect higher oligomers, such as the ones described in previous chapter, the individual differences between the different sub-groups of the oligomeric adducts cannot be discovered. For this reason, structurally precise methods are needed to detect higher oligomers of different adduct groups separately in order to gain new information about their properties and functions in red wine.

1.5 Analysis of proanthocyanidins and their adducts

1.5.1 Analysis of proanthocyanidins by depolymerization

PAs yield anthocyanidins when they are heated in an acidic environment. This property has long been the basis in many of the methods that have traditionally been used in the analysis of PAs, such as the HCl–butanol assay (Swain & Hillis, 1959). Other important methods in the analysis of PAs are phloroglucinolysis and thiolysis, which are extensions of the HCl–butanol assay (Guyot et al., 1998; Kennedy & Jones, 2001). In these methods, nucleophilic reactants are added to the reaction mixture to form adducts with the released extension units of PAs, while the terminal units are released and detected as such. These methods can be used to determine average chain length and sub-unit composition of PAs. The methods are understandably popular because they do not require expensive analytical equipment, but they yield useful information about the concentration and sub-unit composition of PAs. The acid-catalyzed depolymerization assays have also found their applications in the analysis of unique PA adducts in red wine, as mentioned previously (Drinkine et al., 2007a; Zeng et al., 2016).

A modern take on the analysis of PAs using depolymerization was introduced in 2014 when the group-specific UPLC–MS/MS method of Engström et al. (2014) was published. The Engström method has conceptual similarities to phloroglucinolysis and thiolysis in the sense that PAs are fragmented so that the terminal and extension units can be detected separately, which provides information about the concentration and composition of PAs. Beyond the general concept, however, the methods differ considerably. In the Engström method, PAs are fragmented in the ion source of the mass spectrometer by quinone methide fragmentation, which releases the terminal units as such, and the extension units are released as oxidized fragments with mass difference of 2 Da compared to the terminal units (Friedrich et al., 2000). Then, the extension and terminal units are detected by selected reaction monitoring (SRM), which provides both sensitivity and specificity. The in-source fragmentation is achieved by utilizing collision-induced dissociation (CID) and a set of increasing cone voltages (CV) that were optimized to efficiently fragment PAs of various sizes.

The Engström method has three major advantages over the methods based on chemical degradation. First, considerable time saving is achieved because the PA-containing samples can be analyzed with the UPLC–MS/MS instrument as such without first having to do the chemical degradation of PAs separately. Second, the fragmentation of PAs is done after their chromatographic separation, which means that information about the composition of intact PAs is imprinted to the shapes of the chromatograms. The chromatographic profiles often have complex shapes because numerous PAs are detected, and PAs always exist as complex mixtures. Therefore, the chromatographic profiles can be referred to as two-dimensional (2D) chromatographic fingerprints (Salminen, 2018). Third, the chromatographic separation and mass spectrometric detection provide selectivity and they reduce the need for sample pre-treatments before the analyzes, albeit it does not remove it completely in all cases. The Engström method is not without its limitations though, and in its current version the proportions of the epimeric constituting units (catechin and epicatechin; gallocatechin and epigallocatechin) cannot be determined from PAs, unlike with phloroglucinolysis and thiolysis. The group-specific UPLC–MS/MS methodology is also suitable for analysis of common monomeric polyphenols, like flavonoids (Engström et al., 2015). In that case, glycosidic flavonoids are fragmented in the ion source with suitably high CVs, and the released aglycones are then detected using multiple reaction monitoring (MRM).

1.5.2 Applying group-specific analysis to oligomeric adducts

One of the primary hypotheses leading to this thesis was that the PA–Mv adducts in red wine could be detected using group-specific UPLC–MS/MS methodology similarly to PAs. Indeed, the three major groups of PA–Mv adducts in red wine (Figure 3) have been shown in numerous occasions to produce certain fragments in mass spectrometric analysis that satisfy the essential requirements for group-specific analysis (Pati et al., 2006; Sánchez-Ilárduya et al., 2014; Zeng et al., 2016). These basic requirements are that the fragment ions would need to be created regardless of the chain lengths of the adducts, the exact compositions of the PA moieties, e.g., the hydroxylation pattern of the B-ring, and regardless of the glycosidic units attached to the malvidin aglycones. The potential fragment ions for PA–Mv^+, PA–methylmethine–Mv^+ and PA–Mv–FL adducts are hydroxyvinylmalvidin, vinylmalvidin and 6-methylenemalvidin, respectively (Figure 4). Because the promising fragment ions are not simply extension or terminal units, they will be referred to as quantification markers or quantification marker ions. These marker ions could be detected in similar manner as PAs in the Engström method, i.e., the marker ions would first be produced by in-source CID and then detected by MRM. Should the hypothesis be correct and method development successful, completely

novel information could be obtained about the basic properties of PA–Mv adducts because both quantitative and qualitative information could be obtained with structural precision at a compound group level.

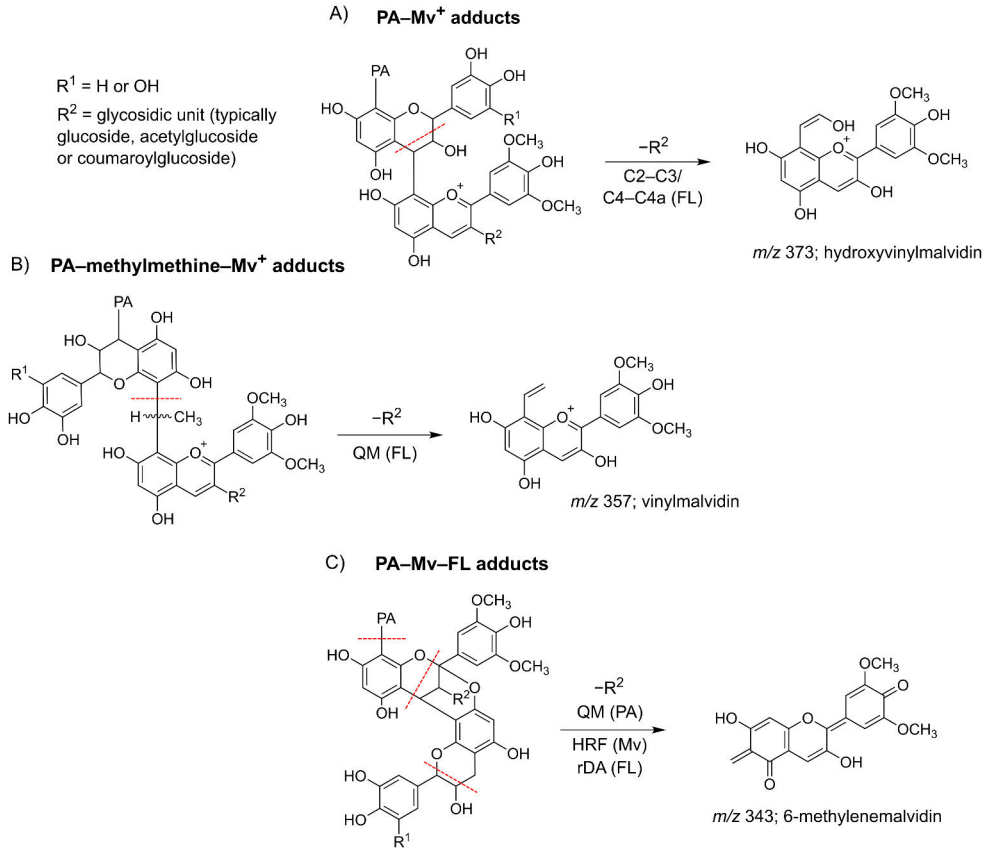

Figure 4. Proposed quantification marker ions for three groups of proanthocyanidin–malvidin glycoside adducts found in red wine, and their formation mechanisms. The red dashed lines represent which parts of the adducts are fragmented to produce the marker ions. The fragmentation mechanisms are presented with the abbreviations and the structural moieties where the fragmentations happen are indicated in the parentheses. Information for this figure was compiled from Zeng et al. (2016), Pati et al. (2006) and Sánchez-Ilárduya et al. (2014). The figure was adapted from Article I with the permission from the copyright holder. Abbreviations: FL, flavan-3-ol; HRF, heterocyclic ring fission; Mv, malvidin glycoside; PA, proanthocyanidin; QM, quinone methide; rDA, retro Diels–Alder.

The group-specific UPLC–MS/MS methodology was expected to be suitable for the analysis of anthocyanins and monomeric adducts of anthocyanins in red wine as well. Suitable quantification markers for the monomeric compound groups would be their aglycones, i.e., the glycosidic units would be cleaved off by in-source CID and

the aglycones would then be detected by MRM. The monomeric pigment groups were targeted as well, because the vision leading to this project was to develop group-specific UPLC–MS/MS method that could provide extensive information about the main adduct composition of red wine. While the true novelty was expected to come from the detection of PA–Mv adducts, it was thought to be important to supplement their detection with the detection of anthocyanins and their monomeric adducts.

1.6 Aldehyde-mediated polymerization of flavonoids

The motivation for studying the reactivity of PAs, FLs and anthocyanins with aldehydes has typically been to gain better understanding about the potential impact of the formed products on the sensorial properties of red wine, and mainly to colour and astringency (Es-Safi, Le Guernevé, et al., 2000; Guo et al., 2017; Nonier Bourden et al., 2008; Pissarra et al., 2003; Sheridan & Elias, 2015; Teng et al., 2019; Wang et al., 2022). In these studies, synthesis experiments have been performed with both monomeric starting materials and PA mixtures, and acetaldehyde additions have even been done directly to red wines. In a more general context, polymerization reactions between phenols and formaldehyde have had commercial usage since the early 1900s, and the resulting polymers were the first fully synthetic and commercially successful resins or plastics (Gilbert, 2016). Mechanistically, acid-catalyzed phenol–formaldehyde polymerization occurs similarly as the formation of PA–methylmethine–Mv^+ adducts in red wine (Heath, 2017). Additionally, the phenol–formaldehyde polymerization can take place by base catalyst as well. Phenol–formaldehyde resins have been used at industrial level to obtain adhesives, laminates, coatings, and foams, for example (Vera & Urbano, 2021). Recently, PAs and FLs have been studied to replace phenol as starting material due to their bioavailability and biodegradability, for instance, which are nowadays desired properties in green chemistry (Vera & Urbano, 2021).

Aldehyde-mediated polymers of FLs have been studied for their biological properties outside the context of red wine in only few instances. One such study was conducted by Chung et al. (2004), who studied antioxidant properties of catechin–acetaldehyde polymers. Another study was conducted by Kim et al. (2004), who studied inhibition effects of catechin–acetaldehyde polymers on the proteinases that cause proteolytic degradation of extracellular matrix. Overall, studies regarding the biological properties of aldehyde-mediated FLs or PAs are scarce in the literature, and especially scarce are detailed structure–activity studies.

Polymerization of FLs provides an appealing way to synthesize polymers from monomers, but also to artificially increase the chain length of natural PA mixtures. The degree of polymerization of PAs is a key feature affecting the well-known

property of PAs, namely, the ability to bind to proteins and precipitate them (Leppä et al., 2020; Ropiak et al., 2017; Zeller et al., 2015). The PA–protein interactions give rise to useful biological properties in potential applications in agriculture, such as anthelmintic activity against gastrointestinal nematodes in ruminants (Mueller-Harvey et al., 2019). Importantly, the biological properties of aldehyde-mediated oligomers of FLs or PAs have not been studied in detail in this context before, and this literature background partly led to the conceptualization of Article V.

The aim in Article V was to hemisynthesize aldehyde-mediated dimers of catechins (Figure 5), which were dubbed as PC analogs, and to compare their biological properties to the properties of natural PC oligomers. Dimers were synthesized to enable direct structure–activity comparison against natural PC oligomers, and to gain information about the properties of smallest possible PC analogs before proceeding to study higher oligomers. The hemisynthesis of PC

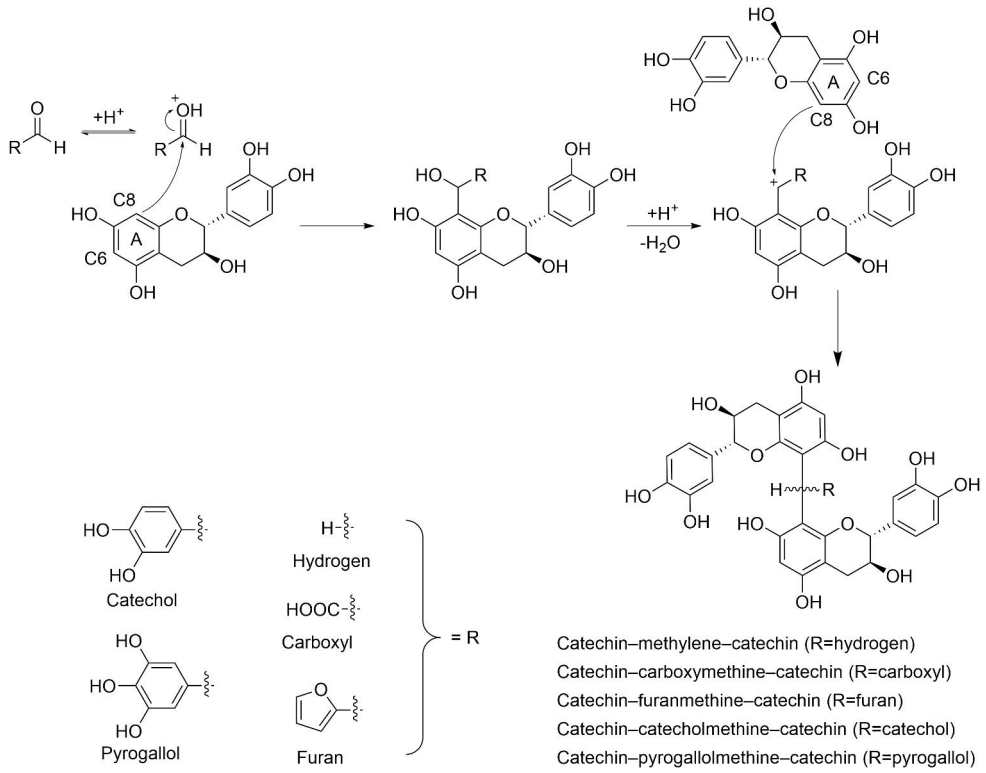

Figure 5. Reaction mechanism and structures of the hemisynthesized catechin-based PC analogs. Similar PC analogs were synthesized from epicatechin as well. The reaction mechanism was adapted from Es-Safi et al. (2002), and the same mechanism also produces the methylmethine-linked adducts of proanthocyanidins and malvidin glycosides found in red wine (Figure 3B).

analogs was inspired by the chemistry of red wine, and the PC analogs were synthesized with the same mechanism that also yields the PA–methylmethine–Mv^+ adducts in red wine (Figure 5). The three properties of the PC analogs that were to be measured were the protein precipitation capacity (PPC), octanol–water partition and stability in phosphate-buffered saline (PBS). The PPC was the main focus due to its linkage to the above-mentioned ruminant-related bioactivities. The PPC of PC analogs was expected to be better than the PPC of corresponding PC oligomers, and further discussion about this hypothesis is provided in results and discussion.

1.7 Aims of the thesis

The main aims of this thesis were to

1. Develop a new group-specific UPLC–MS/MS method that could provide a comprehensive and accurate picture of the main pigment composition of any red wine with a minimal sample pre-treatment. The main emphasis was on the oligomeric PA–Mv adducts (Article I).
2. Analyze commercial red wines with the developed UPLC–MS/MS method to study the composition and evolution of oligomeric PA–Mv adducts (Article III).
3. Find connections between key sensorial properties of red wine, i.e., the colour intensity and sensorially evaluated tannin content and the measured composition of PAs and oligomeric PA–Mv adducts (Articles II and IV).
4. Utilize red wine inspired hemisynthesis to prepare PC analogs and study their protein precipitation capacity and other properties (Article V).

This thesis will cover the key results of Articles I–V using selected examples while the detailed results and discussion will be left to the individual articles. The focus of this thesis will be on the oligomeric and polymeric compound groups in red wines, and especially on PA–Mv adducts.

2 Materials and Methods

2.1 Red wines

The red wines utilized in Article I and part of the red wines utilized in Articles II–IV were purchased by the Natural Chemistry Research Group (NCRG) or by individual members of NCRG (n=45). For Articles II–IV, 272 commercial red wines were provided by Alko Inc., which is a Finnish company owned by the State of Finland. Alko Inc. has a monopoly on selling alcoholic beverages in Finland that contain alcohol more than 5.5%. An aliquot of 6 ml was sampled from each red wine provided and the samples were stored at −80 °C. The whole wine set (n=317) is briefly summarized in Table 1. Sub-sets of the whole wine set were utilized for different purposes in Articles I–IV, and the utilized sub-sets are specified separately in each case in the corresponding articles.

Table 1. Summary of all red wines (n=317) used in Articles II–IV. The numbers in parentheses are numbers of wines in each category. Three or more grape varieties were used in 94 wines. The table was adapted from Article I with permission from the copyright holder.

Countries	Regions	Primary Grape varieties	Secondary Grape varieties	Age in years
France (90)	Douro (40)	Pinot Noir (52)	None (176)	1 (78)
Portugal (46)	Languedoc-Roussillon (30)	Shiraz (48)	Touriga Franca (29)	2 (71)
Australia (40)	Beaune (24)	Merlot (39)	Cabernet Sauvignon (23)	3 (44)
Italy (32)	Pfalz (19)	Cabernet Sauvignon (31)	Merlot (14)	4 (28)
Germany (20)	South Eastern Austarlia (19)	Touriga Nacional (29)	Zweigelt (13)	5 (11)
Spain (19)	Listrac-Medoc (18)	Blaufrankisch (13)	Tinta Amarela (11)	≥ 6 (8)
USA (15)	Barossa Valley (15)	Tempranillo (11)	Shiraz (9)	not known (77)
Others (55)	Others (152)	Others (94)	Other (42)	

2.2 Sephadex LH-20 Fractionation

Three of the red wines used in Article I were fractionated with Sephadex LH-20 gel chromatography. These wines were J.P. Chenet Merlot (France, Languedoc-Roussillon, 2015), Hardys VR Cabernet Sauvignon (Australia, South Eastern Australia, 2013) and Piedemonte Reserva (mix of Merlot, Tempranillo and Cabernet Sauvignon grapes; Spain, Navarra, 2011). Ethanol was first evaporated using rotary evaporator, and the remaining water phases were frozen and freeze-dried. The freeze-fried residues were dissolved to ultra-pure type I water, filtered through 0.2 µm PTFE filters, and loaded on to a glass column (320×55 mm; Chromaflex, Kimble-Chase Kontes, Vineland, NJ, USA) that was packed with Sephadex LH-20 material (GE Healthcare, Uppsala, Sweden). The Sephadex material was stabilized with water prior to loading the samples. Ten fractions were eluted with water and mixtures of water, methanol, and acetone, and the volume of each fraction was 500 ml. The elution protocol is described in Article I. The organic solvents were evaporated by leaving the fractions in open containers in fume hoods overnight and the remaining water phases were frozen and lyophilized.

2.3 Analytical chromatography and mass spectrometry

Three different Acquity ultra-performance liquid chromatography (UPLC) systems from Waters were utilized with different detector setups (Waters Corporation, Milford, MA, USA). The UPLC systems were composed of a binary solvent manager, a sample manager, column oven, and diode array detector (DAD). UV–Vis data was recorded between 190 nm and 499 nm. Two different columns were utilized, and both were Acquity UPLC BEH phenyl columns (2.1 mm i.d., 1.7 µm) but with different lengths (100 mm and 30 mm; Waters Corporation, Wexford, Ireland). Acetonitrile (A) and 0.1% aqueous formic acid (B) were used as eluents and the gradients are described below separately for each setup. The injection volume was always 5 µl (full loop).

2.3.1 UPLC-DAD-ESI-TQ-MS

One UPLC system was attached to a Xevo Triple Quadrupole (TQ) mass spectrometer (Waters Corporation, Milford, MA, USA). This system was used in Articles I–IV. The ion source (electrospray ionization, ESI) was operated in both negative and positive ion modes depending on the utilized method. In both cases, the ion source was operated with the following parameters: capillary voltage was 3.4 kV, ion extractor voltage 3 V, source temperature 150 °C, desolvation temperature 650 °C, desolvation gas flow rate 1000 l h^{-1} and cone gas flow rate 100 l h^{-1}. Nitrogen

was used as desolvation and cone gasses, and argon was used as a collision gas. A 100 mm BEH phenyl column was always used with this setup and the flow rate of the eluent was 0.5 ml min^{-1} with the following gradient: 0–0.5 min: 0.1% A and 99.9% B; 0.5–5 min: 0.1–30% A and 99.9–70% B (linear gradient); 5–8 min: 30–45% A and 70–55% B (linear gradient); 8–11.5 min: column wash (90% A and 10% B) and stabilization (0.1% A and 99.9% B). The temperature of the column oven was 40 °C. The UPLC system was operated with MassLynx software (version 4.2 SCN982; Waters Corporation).

2.3.2 UPLC-DAD-HESI-Q-Orbitrap-MS

The second UPLC system was coupled to a Q Exactive Orbitrap mass spectrometer (Thermo Fisher Scientific GmbH, Bremen, Germany). This system was used in Articles IV and V. The ion source (heated electrospray ionization, HESI) was operated in negative ion mode, and the capillary voltage was −3 kV. The capillary temperature was set at 380 °C, and the flow rates of the sheath and auxiliary gasses (N_2) were 60 and 20 arbitrary units, respectively. The auxiliary gas heater temperature was 300 °C in Article V and 0 °C in Article IV. The S-lens RF level was 60, the resolution of the full scan analyzes was 70 000, the automatic gain control was 1×10^6, and maximum injection time was 100 ms. Only the 100 mm phenyl column was used with this setup. In Article IV, the gradient was the same as described in chapter 2.3.1. In Article V, the gradient was identical to the one described in chapter 2.3.1 until 5 minutes, after which the column was washed (90% A and 10% B) and stabilized (0.1% A and 99.9% B) between 5–8.5 minutes. The temperature of the column oven was 40 °C. The MS system was calibrated using Pierce ESI Calibration Solutions (Thermo Fischer Scientific Inc., Waltham, MA)

2.3.3 UPLC-DAD

DAD was the only detector in the third UPLC system, and this setup was only used in Article V. A 30 mm BEH phenyl column was used, and the flow rate of the eluent was 0.65 ml min^{-1}. The gradient was as follows: 0–0.1 min: 3% A and 97% B; 0.1–4 min: 3–50% A and 97–50% B; 4–5.5 min: column wash (90% A and 10% B) and stabilization (3% A and 97% B). The temperature of the column oven was 40 °C.

2.4 Semipreparative HPLC-DAD

The semipreparative HPLC system used in Article V was from Waters (Waters Corporation, Milford, MA, USA). The system consisted of 2535 Quaternary Gradient Module, 2998 Photodiode Array Detector and a Fraction Collector III. A

C18 Gemini column from Phenomenex with particle size of 10 µm and pore size of 110 Å was used (Phenomenex, Torrance, CA, USA). The dimensions of the column were 150×21.2 mm, and the internal diameter was 4.6 mm. Acetonitrile (A) and water (B) were primarily used as eluents, and the gradients were optimized separately for each purified compound based on their retention times on the UPLC systems (chapters 2.3.2. and 2.3.3.). In two cases, 0.1% aqueous formic acid was used instead of water as the eluent B. The flow rate of the eluent was 8 ml min^{-1}. All samples were filtered through 0.2 µm PTFE filters before injections and the injection volume was 5 ml (full loop).

2.5 Method development for detection of anthocyanin adducts

The instrumentation described in chapter 2.3.1 was utilized in the method development for detection anthocyanins and their adducts throughout, and the MS system was operated in the positive ion mode. Dozens of anthocyanins, monomeric anthocyanin adducts and oligomeric PA–Mv adducts were characterized with product ion scans from the Sephadex LH-20 fractions (chapter 2.2.). Product ion scans were performed separately for both the molecular ions and for the product ions that were to be used as quantification markers, i.e., the aglycones of the monomeric pigments and the malvidin-derived moieties of the PA–Mv adducts (Figure 4). The data of the compound characterization is presented in Article I.

The MRM methods were optimized by performing multiple MRM analyses with the Sephadex LH-20 fraction and intact model wines by changing the parameters of the methods one at a time. First, three most abundant product ions were chosen for each quantification marker ion based on the product ion scans. Their collision energies (CEs) were optimized by increasing the energies in 3 eV increments. Only the Sephadex LH-20 fractions were used in the CE optimizations. A rough estimate of a decent CV was used at this stage of the optimization. The two most abundant products ions were chosen for the quantitative and qualitative transitions. Then, the CVs were optimized using the quantitative transitions. The CV was increased in 7 V increments in the optimization of the method for the monomeric compounds, and in 10 V or 20 V increments in the optimization of the method for the oligomeric adducts because a wider range of voltages needed to be tested. The CVs of the monomeric pigment groups were optimized by using the model compounds in the Sephadex LH-20 fractions and, additionally, several model wines were utilized as such in the optimization of the CVs for the PA–Mv adducts. Total areas of the hump-like chromatograms of the PA–Mv adducts were measured from the model wines as function of CV, and changes in the profiles of the chromatograms were visually evaluated to support the CV optimization for the PA–Mv adducts.

The methods were validated for their intra-run repeatability, carryover and for the ratios of the quantitative and qualitative transitions. Unprocessed model wines were analyzed repeatedly for the method validation. Calibration curves were prepared from a single reference wine, the J.P. Chenet Merlot (France, Languedoc-Roussillon, 2015), to quantify the concentrations of the analytes as relative proportions of those in the model wine. In other words, the concentration of each pigment group in the reference wine was defined to be 100% and the quantified concentrations in other wines were obtained as percentage values via calibration curves. A second wine, Alamos Tempranillo, was used as an external standard to correct the raw responses. More details about the quantification process is provided in the next chapter 2.6.1. The parameters of the methods and the validation data are presented in Article I, along the information of the model wines.

2.6 Analysis of the red wines

2.6.1 Analysis of PA–Mv adducts and monomeric pigments

All red wines (n=317) were analyzed with the method developed in Article I using the instrumentation described in chapter 2.3.1, and the data was used in Articles II–IV. Only the quantitative transitions of the method were used in these analyses. The concentrations of the pigment groups were obtained as relative proportions of the concentrations in the reference wine, as described in chapter 2.5. The concentrations of the PA–Mv adducts were calculated from the summed areas of the small oligomeric adducts (SOAs), medium-sized oligomeric adducts (MOAs) and large oligomeric adducts (LOAs) to obtain a metric for the total concentrations. The proportions of the SOAs, MOAs and LOAs of the summed total areas were calculated as well (SOA-%, MOA-% and LOA-%) to obtain metrics, which described the size-distribution of the PA–Mv adducts between wine samples (Figure 6).

The external standard wine, Alamos Tempranillo 2015, was analyzed periodically after every 10 injections to account for the fluctuation in the performance of the mass spectrometer. The responses of malvidin glycosides were monitored in the external standard to correct the raw responses of malvidin, cyanidin and delphinidin glycosides, and petunidin glycosides were used to current the raw responses of petunidin and peonidin glycosides. Carboxypyranomalvidins were monitored to correct the responses of all carboxypyranoanthocyanins, and methylpyranomalvidins and B-type vitisins (Figure 2A). Phenylpyranomalvidins were monitored to correct the responses of all pinotin-type malvidin adducts (Figure 2B). Each of the three PA–Mv adduct groups were used to adjust the responses of the corresponding groups.

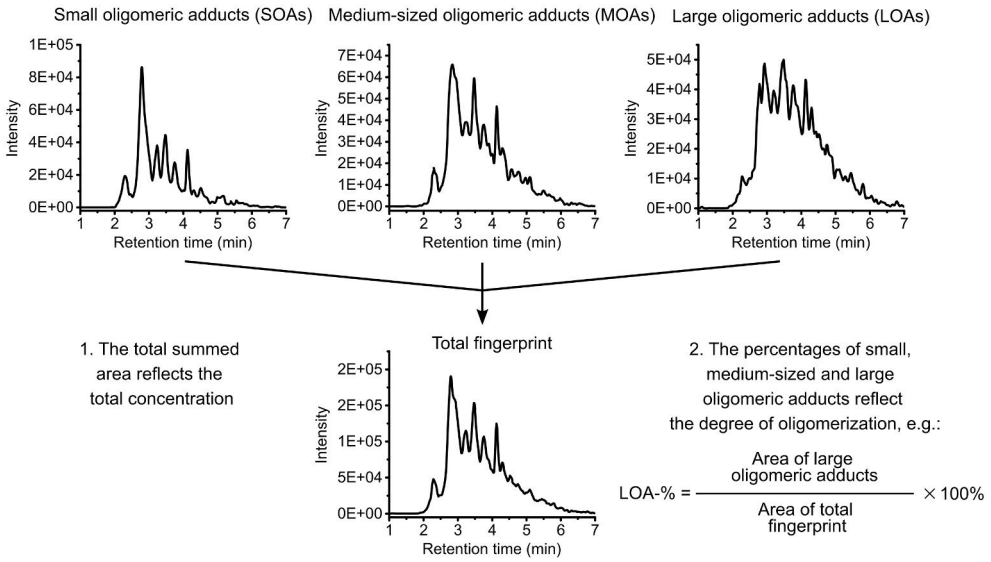

Figure 6. Example of the calculation of numerical results from 2D fingerprints of the proanthocyanidin–malvidin glycoside adducts. The chromatogram areas of small, medium-sized and large oligomeric adducts (SOA, MOA and LOA, respectively) are summed to obtain total area, which is further transformed to relative concentration using a calibration curve. The proportions of SOA, MOAs and LOAs of the total area are calculated to obtain metrics that describe the size-distribution of the adducts between wine samples. In other words, relative information about degree of oligomerization is obtained via the proportions of SOAs, MOAs and LOAs. The figure was adapted from Article II with permission from the copyright holder.

2.6.2 Analysis of proanthocyanidins and other polyphenols

All red wines were analyzed with the UPLC–MS/MS method of Engström et al. (2014, 2015) using the instrumentation described in chapter 2.3.1, and the data was used in Articles III and IV. The PC and PD units were detected with three different CVs, and their concentrations were calculated from the summed total areas of the produced PC and PD fingerprints. Sephadex LH-20 fractions prepared from *Tilia* flowers (PC-rich fraction) and *Ribes nigrum* leaves (PD-rich fraction) were used as quantification standards. The equation for the calculation of the mDP of the PAs was calibrated using six Sephadex LH-20 fractions produced from extracts of *Vaccinium vitis-idaea*, *Calluna vulgaris*, and *Tilia* with known mDPs. The concentrations of catechin, epicatechin, gallocatechin and epigallocatechin were quantified with the Engström method using corresponding commercial standards. The Engström method was also used detect and quantify quercetin, myricetin, hexahydroxydiphenoyl (HHDP) and galloyl derivatives, and the total phenolic content of the wines was measured using a modified Folin–Ciocalteu method (Salminen & Karonen, 2011).

However, these results are not covered in this thesis, but details about these analyses can be found in Article IV.

2.6.3 Colour intensity and sensorially evaluated tannicity

The colour intensity of all red wines was measured with a well-plate reader (Multiskan Ascent, Thermo Fisher Scientific, Waltham, USA) and 96-well plates (Article II). The absorbances were measured at 415, 520 and 620 nm and the summed absorbance was used as a metric for colour intensity. The measurements were done in duplicates from undiluted wines.

Out of the 272 wines that were provided by Alko Inc., the perceived tannin content (tannicity) was sensorially evaluated from 201 wines at Alko Inc. (Article IV). Tannicity was defined as the drying sensation in the mucous membrane in mouth that could also be felt also with a delay after expectoration. The evaluations were done by a tasting group consisting of approximately 30 employees of Alko Inc., and each member had to demonstrate their suitability and expertise in sensorial analysis before they got to join the tasting group. The sensorial analysis group receives regular training about sensorial analysis, but they were not specifically trained for evaluating the tannicity of these particular red wines. The sensorial evaluations were discriminant-type evaluations, and the wines were categorized as either “tannic” or “medium tannic”. The former group was the one perceived to have more tannins. Each wine was tasted by three or four persons. Their combined evaluations had to be unanimous or otherwise the wine could be re-evaluated before deciding the final classification. Alko Inc. only provided the final classification, and no information about the panelists, their identity, or their individual evaluations were provided, which ensured their complete anonymity. The tannicity classifications could be considered as public information because Alko Inc. lists the tannicity classifications for wines in their selection in their web page at www.alko.fi.

2.7 Hemisynthesis of procyanidin analogs

Ten different PC analogs were synthesized from catechin and epicatechin with five different aldehydes (Figure 5; Article V). The aldehydes were formaldehyde, glyoxylic acid, furfural, 3,4-dihydroxybenzaldehyde (3,4-DBA) and 3,4,5-trihydroxybenzldehyde (3,4,5-TBA). The syntheses were done in a 10 ml boiling flask, which was placed in water bath at 45 °C. The solvent was 15% aqueous methanol. The pH of the solvent was adjusted to 2.5 using formic acid except when glyoxylic acid was used as a starting material. In that case, the starting material functioned as the catalytic acid as well, and the pH of the reaction mixture was approximately 2.5. The concentration of catechin and epicatechin was always 45

mM, while the concentrations of formaldehyde and furfural were 90 mM, the concentration of glyoxylic acid was 22.5 mM, and the concentrations of 3,4-DBA and 3,4,5-TBA were 45 mM. Copper(II)sulfite was added to the reaction with glyoxylic acid (1.5 mM) to introduce Cu^{2+} ions to catalyze the reaction. The reactions were monitored using the UPLC–DAD system (chapter 2.3.3.), and the reactions were stopped by cooling the reaction vessel in an ice bath. The main dimeric products were isolated using semipreparative HPLC–DAD (chapter 2.3.4.) and the compounds were identified based on their accurate masses and the corresponding molecular formulae (chapter 2.3.2.), UV–Vis spectra, and by NMR spectroscopy (chapter 2.8).

2.8 NMR spectroscopy

The measurements were done with Bruker Avance-III 500 spectrometer that was equipped with a Smartprobe (BB/1H; Fällanden, Switzerland) operating at 500.08 MHz for ^{1}H, and at 125.76 MHz for ^{13}C. The samples were dissolved in acetone-d_6 in approximately 5 mM concentrations, and the samples were kept at 5 °C during the measurements to prevent degradation of the compounds. The following experiments were performed: ^{1}H (zg30), ^{13}C (zgpg30), COSY (cosygpmfphpp), HSQC (hsqcedetgpsisp2.3) and HMBC (hmbcetgpl3dn). J_{CH} was set to 145 Hz for the HSQC experiments and the J_{CH} range to 120-170 Hz, and the long range J_{CH} was set to 8 Hz for the HMBC experiments.

2.9 Measurement of biological properties of procyanidin analogs

Three different experiments were done to evaluate the biological properties and activities of the PC analogs and the reference compounds. The reference compounds were PC dimers B2 and B3, PC trimer C1, epigallocatechin-3-*O*-gallate (EGCG), and the starting materials catechin and epicatechin.

2.9.1 Protein precipitation capacity

PPC was measured using a turbidimetric well-plate reader assay of Engström et al. (Engström et al., 2019) where the PC analogs and reference compounds reacted with BSA resulting in haze formation. The abundance of the forming haze was measured as absorbance at 420 nm. The absorbance was measured every minute for half an hour, and the plates were shaken before each measurement. The maximal absorbance was recorded from the kinetic data and it was used as a measure for the PPC. The concentration of BSA was always 0.1 mM in the reaction mixture, and the

concentrations of the PC analogs and the reference compounds were 0.25 mM, 0.65 mM, 1.05 mM, 1.45 mM, 1.85 mM and 2.25 mM. The measurements were done in triplicates (or in duplicates in the case of the PC trimer C1), and 75 µl of stock solutions of BSA and PC analogs or reference compounds were pipetted to each well. The background absorbance was measured once at each concentration from a solution containing all other components except the BSA. The PC analogs and reference compounds were dissolved to water, and BSA was dissolved to a pH 5 buffer containing sodium acetate (50 µM) and ascorbic acid (60 µM). Finally, the supernatants were analyzed by UPLC–DAD (chapter 2.3.3) to quantify the remaining compounds in the supernatant according to Engström et. al (2022). The proportions of precipitated compounds were calculated to supplement the primary PPC data from the well-plate assay. Details about these analyzes can be found in Article V.

2.9.2 Octanol–water partition

The octanol–water partition was measured using a shake-flask method in 2 ml Eppendorf tubes (Virtanen & Karonen, 2020). The tested compounds (200 µM) were dissolved to 2 ml of water that had been saturated with n-octanol and, after mixing in Vortex mixer, 500 µl aliquots were transferred to new 2 ml tubes. Then, 500 µl of n-octanol that had been saturated with water was added to the new Eppendorf tubes, which were then mixed in Vortex mixer for 2 hours. Both the n-octanol and water phases, including the initial stock water solution, were analyzed using UPLC–DAD (chapter 2.3.3.). The partition coefficient K_{ow} and its logarithm log$P$ were calculated as ratios of the areas in the n-octanol and water phases. The recovery-% was calculated by dividing the summed areas in n-octanol and water phases with the areas in the initial water solution.

2.9.3 Stability in phosphate buffered saline solution

The PBS solution was prepared by dissolving a PBS tablet (Sigma) to ultra-pure water. The sodium and potassium chloride concentrations were 0.137 M and 0.0027 M, respectively. The phosphate concentration was 0.01 M, and the pH was 7.4. Each compound (150 µM) was dissolved to 2 ml of the PBS buffer in an Eppendorf tube, and the solutions were transferred to a 2 ml UPLC vial after mixing the solutions in a vortex mixer. The solutions were then analyzed periodically once in every 47.5 minutes for 13 hours using the instrumentation described in chapter 2.3.2. The peaks of the analytes were integrated from the UV chromatograms (280 nm) until the analytes were no longer distinguishable from background or until the final time point. The integrated peak areas were normalized with the highest areas, i.e., with

the areas in the first injections, and the normalized areas were further ln-transformed to obtain linear fits for linear regression models. Half-lives were calculated from the slope parameters of the regression models. The degradation products were tentatively characterized based on their accurate masses and the corresponding molecular formulae, and based on their UV–Vis spectra.

2.10 Statistical analyzes

All statistical analyzes were performed with R in an integrated development environment, Rstudio (R core team, 2022; Rstudio team, 2022). Several software versions were used ranging from 3.5.3. to 4.2.2. with R, and from 1.2.1335. to 2022.12.0.353. with Rstudio. Ggplot2 package was used in all articles to visualize data (Wickham, 2016). Only the key methods for this thesis are described here, while complete listing of the utilized methods is provided in the original articles.

2.10.1 Regression analyzes

Partial least squares regression analyzes (PLSR) were used in articles II and III to model the multivariate data. The PLSR analyzes were done with the *plsdepot* package (Sanchez, 2012). In article II, the colour intensity was the response variable that was modelled with the concentrations of malvidin glycosides, B-type vitisins, carboxy-, methyl-, phenyl-, catechyl-, and guaiacylpyranomalvidin glycosides, and PA–Mv^+ and PA–methylmethine–Mv^+ adducts. The LOA-% of the PA–Mv^+ and PA–methylmethine–Mv^+ adducts were utilized as predictors as well to model the relative differences in the average sizes of the adducts between wine samples. The variables were log-transformed and scaled to zero means and unit variances before fitting the models. Predicted residual sums of squares, residual sums of squares, coefficient of determination (R^2) and cross-validated R^2 (Q^2) were used to decide the optimal number of latent variables. In article III, the concentrations of PA–Mv^+, PA–methylmethine–Mv^+ and PA–Mv–FL adducts, and their LOA-%, were modelled in 1-year-old wines. The concentrations of PAs, FLs, and malvidin glycosides, and the FL/PA-ratio and the mDP of PAs were used as predictors. Separate model was fitted for each response variable and two latent variables were used in each model. All models in both articles II and III were cross-validated with the leave-one-out method.

Partials least squares discriminant analysis (PLS-DA) was used to model the perceived tannin content, i.e., tannicity with the concentrations of PAs and PA–Mv^+, PA–methylmethine–Mv^+ and PA–Mv–FL adducts, with the mDP and PD-% of PAs, and with the LOA-% of the three groups of PA–Mv adducts. The PLS-DA was done using the *mixOmics* package (Rohart et al., 2017). The number of latent variables were chosen based on the error rates in cross-validation, which was 15-fold cross-

validation that was repeated 50 times. Error rates and the receiver operating characteristics plot were used to evaluate the performance and the fit of the model.

2.10.2 Quantile chromatographic fingerprints

A new purpose-built data visualization tool was developed in Article III to summarize and visualize chromatographic data of the 2D fingerprints from multiple samples simultaneously. Briefly, the fingerprints of SOAs, MOAs and LOAs of the PA–Mv adducts were first summed and then scaled with highest intensity to form a total fingerprint for each compound group and for each selected wine sample. Multiple total fingerprints were then aligned using a parametric time warping algorithm (Bloemberg et al., 2010; Eilers, 2004). Finally, median fingerprint was calculated from multiple aligned total fingerprint to represent a typical fingerprint, and 10^{th} and 90^{th} percentiles were similarly calculated to visualize within-group variation. The whole protocol is described and explained in greater detail in Article III where the individual steps are visually demonstrated in Figure 1 of the article. The protocol was also used in Article IV to summarize and visualize 2D fingerprints of PC and PD containing PAs and other polyphenolic compound groups in red wine, but these results will not be presented in this thesis.

2.10.3 Dose–response models

A four-parameter log-normal dose–response model was fitted to the PPC data from the well-plate reader assay (chapter 2.9.1.) with the *drc* package (Ritz et al., 2015). Different models were first compared using the mselect function to find the best fitting model. The best fit was assessed using Akaike's information criterion, residual errors and log-likelihood. The lower asymptote was assumed to be zero, and the upper asymptote (maximal absorbance) was assumed to be the same with all compounds and this parameter was estimated from the experimental data. The effective dose and slope parameters were not restricted in any way, and they were estimated from the data.

3 Results and discussion

3.1 Development of the multiple reaction monitoring method

3.1.1 Optimization of the method parameters

Sephadex LH-20 fractions and characterization of model compounds

Three model wines were fractionated with Sephadex LH-20 gel chromatography to reduce chemical background in compound characterization and in the optimization of the parameters of the MRM method. Multiple fractions were first analyzed with full scan analyzes using several CVs (Figure 7). The aim was to produce untargeted fragmentation to see which ions would be produced in the highest abundances. The full scan spectra were extracted from the whole range of the chromatograms and the spectra showed numerous common ions that could be attributed to known compounds in red wines. For instance, the molecular ions of the anthocyanidins (*m/z* 287, 301, 303, 317 and 331) could be clearly observed, as well as several ions that could be linked to procyanidins, e.g., *m/z* 579 (PC–PC dimer) and *m/z* 289 (QM fragment of PC–PC dimer; Alberts et al., 2012; Li & Deinzer, 2007). Importantly, these early results demonstrated the production of the hypothesized quantification marker ions (Figure 4) for the PA–Mv adducts at *m/z* 343, 357 and 373.

Overall, 66 model compounds were characterized from the Sephadex LH-20 fractions for the method development. These compounds included anthocyanins and pyranoanthocyanins with glucose, acetylglucose or coumaroylglucose moieties. 23 of the model compounds were dimers and trimers of the PA–Mv^+, PA–methylmethine–Mv^+ and PA–Mv–FL type adducts, i.e., all major branches of the first generation of adducts were covered. The complete list of the characterized model compounds is presented in Article I.

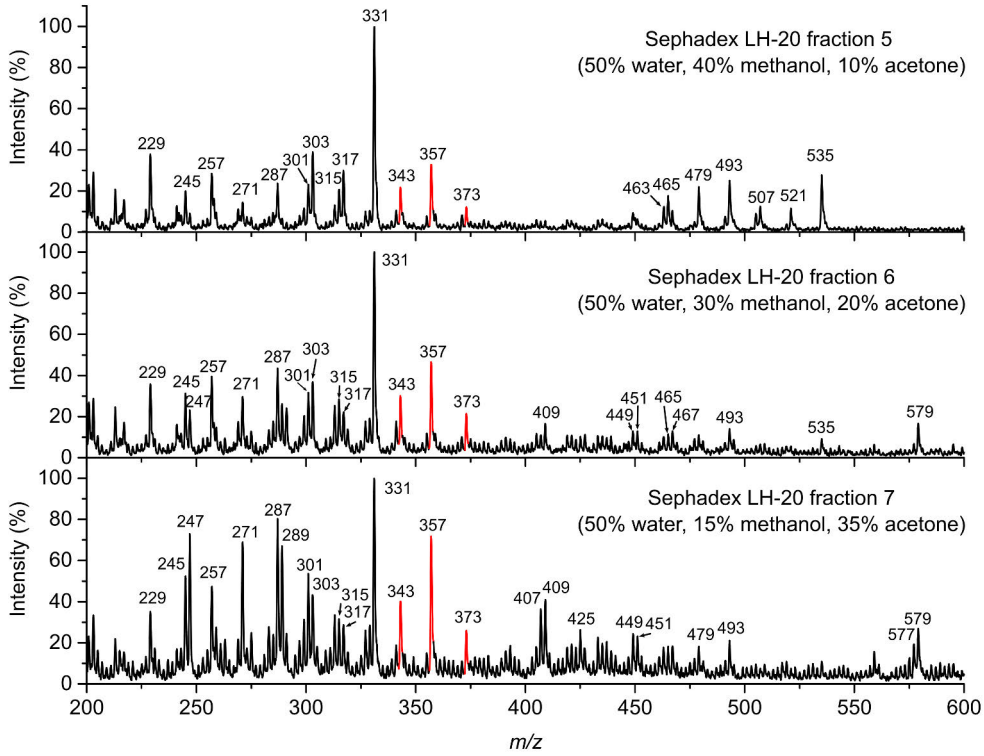

Figure 7. Full scan mass spectra of three Sephadex LH-20 fractions from J.P. Chenet Merlot wine in positive ion mode. The cone voltage was 140 V with the purpose of producing untargeted fragmentation. The marker ions proposed for the three groups of proanthocyanidin–malvidin glycoside adducts in Figure 4 are coloured in red. The figure is adapted from Article I with the permission of the copyright holder. Refer to Article I for similar figures from the Hardys VR Cabernet Sauvignon and Piedemonte Reserva wines.

Method optimization for the monomeric pigments

As with any MRM method, the key parameters to be selected and optimized were the *m/z* values of precursor and product ions, CV in the ion source and CE in the collision cell. The optimization of the MRM method for the monomeric pigments was straightforward because it was possible to find a single set of parameters that were suitable in the production and detection of the quantification marker ions with all model compounds within a compound group. A small increase in the optimal CV was found as the glycosidic units increased in molecular weight, but the increases in the optimal voltages were minor. The fragmentation of the produced markers ions in the collision cell was independent of the origin of the quantification marker. In other words, malvidin aglycone always fragmented in same way as function of CE whether the aglycone was produced in the ion source from a malvidin glucoside or malvidin

coumaroylglucoside, for instance. MRM transitions were optimized for all five anthocyanin groups in red wine (Figure 1) and for the corresponding carboxypyranoanthocyanins, except the carboxypyranocyanidins. Compound specific methods for carboxypyranocyanidin glucoside, acetylglucoside and coumaroylglucoside were optimized instead because the group-specific method was not sensitive enough for analysis of red wine. Additionally, MRM transitions were optimized for methylpyranomalvidins, B-type vitisins, phenylpyranomalvidins, catechylpyranomalvidins and guaiacylpyranomalvidins (Figure 2). Refer to article I for the optimized parameters of the MRM transitions and for the optimization data of the CVs.

Method optimization for the oligomeric PA–Mv adducts

As with the monomeric pigments, a single CE could be chosen for each MRM transition with the quantification marker ions for the PA–Mv adducts. However, it was evident that several CVs would be needed for the production of the quantification markers from the PA–Mv adducts to obtain as comprehensive picture of the adduct composition as possible. The glycosidic unit did not affect the optimal CV as much as the degree of oligomerization did. Trimers required typically 30–40 V higher CV for the optimal accumulation of the quantification marker ions compared to corresponding dimers, whereas the effect of the acylation of the glycosidic unit was 10–15 V with the dimers (Figure 8A). This was an expected result because similar results were previously obtained in the development of the Engström method (2014). Engström et al. (2014) observed that the optimal CV in the production of extension and terminal unit ions from PAs increased as the degree of oligomerization increased. Mechanistically, the excess internal energy acquired in CID can disperse over wider area in a larger molecule, which leads to less fragmentation (Gross, 2017b), and an increase in the degree of oligomerization increases the size more than increase in the size of the glycosidic unit. Therefore, higher voltage and more kinetic energy is needed to ensure efficient production of the quantification markers from higher oligomers.

Thus far, only the individual model compounds in the Sephadex fractions were utilized in the optimization of the MRM transitions. However, 13 unprocessed red wines were additionally utilized in the CV optimization for the PA–Mv adducts. Both the areas and the profiles of the chromatograms obtained with the quantitative MRM transitions were monitored as function of CV (Figures 8B and 8C). The chromatogram areas increased in most wines when CV was increased above the optimal voltages for the trimers, which indirectly proved that higher oligomers had to exist in the model wines (Figure 8B). Additionally, the overall shapes of the chromatograms became increasingly more dominated by the chromatographic

humps and the proportions of individual peaks diminished as CV was increased (Figure 8C).

Three different CVs were eventually chosen for each PA–Mv adduct group. The voltages were chosen so that each produced 2D fingerprint was emphasizing differently sized adducts in different proportions. The first CVs were selected to emphasize the smallest adducts, i.e., the dimers (Figure 8A). The second set of CVs was chosen so that they emphasized medium-sized adducts, which was achieved by selecting voltage slightly above the optimal value for the trimers (Figure 8A). The third set of CVs was selected to emphasize the highest oligomers that could be detected with the utilized methodology and instrumentation. This selection was

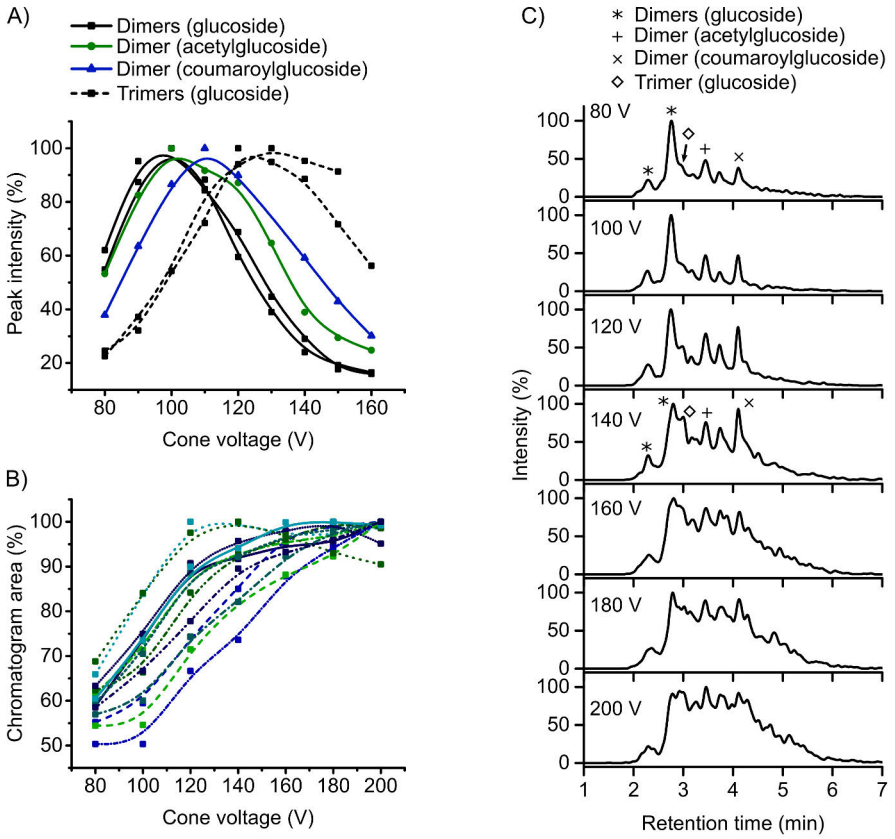

Figure 8. Optimization of the cone voltage of the multiple reaction monitoring method for the PA–Mv^+ adducts. The optimal voltages for the individual oligomers (A) were measured from the Sephadex LH-20 fractions, and 13 model wines were analyzed as such to measure the effect of the cone voltage on the chromatogram areas (B) and on the chromatographic profiles (C). Refer to article I for the optimization data for the other two groups of PA–Mv adducts, and for the optimization data for the monomeric pigment groups. This figure was adapted from Article I with the permission from the copyright holder.

based on achieving the maximal chromatogram areas in the model wines and by visually inspecting the profiles of the chromatograms for the cleanest hump-like profiles (Figure 8B and C). The fingerprints obtained with the different CVs are referred to as small, medium-sized and large oligomeric adducts (SOAs, MOAs and LOAs, respectively). The parameters of the MRM transitions are listed in Article I.

It is important to note that the fingerprints of SOAs, for instance, do not strictly consist only of the dimers. Instead, the dimeric compounds are the most emphasized in the SOA fingerprints when compared to fingerprints of MOAs and LOAs, while higher oligomers are already visible as well but in lesser proportions. On the other hand, the higher oligomers are most efficiently detected and most emphasized in the LOA fingerprints, but the higher oligomers are already visible in smaller abundance in the fingerprints of MOAs and SOAs. The SOA, MOA and LOA fingerprints should not be thought as uncorrelated fingerprints without any overlapping, but rather as three components that together form the bigger picture of the detected compound composition. This rationalization is displayed in the way that the quantitative data of the fingerprints is processed (Figure 6). As described in materials and methods in chapter 2.6.1., the areas of the SOA, MOA and LOA fingerprints are summed and only the summed area is then transformed to relative concentration via a calibration curve. Naturally, the same approach is used with the reference wine when constructing the calibration curves. Additionally, the proportions of the SOAs, MOAs and LOAs of the total summed area are calculated (SOA-%, MOA-% and LOA-%; Figure 5). As can be seen in Article III, and in the method optimization data in Article I, these proportions vary between different wine samples. Based on the theory of the method, this variation is linked to variation in the average sizes of the adducts. Therefore, the SOA-%, MOA-% and LOA-% metrics are also referred to as size-distribution parameters in this thesis. Finally, the purpose of the chosen naming convention was to make it easier to discuss and refer to the different fingerprints, while still being informative about the relative differences between the fingerprints. Analogous naming convention has previously been used by Harbertson et al. who referred to small polymeric pigments (SPP) and large polymeric pigments (LPP) in their precipitation assay (Harbertson et al., 2003), which served as inspiration for the chosen nomenclature.

3.1.2 Method validation

One of the most important features to validate in a group-specific method is specificity. The method development was based on a few model compounds, but the resulting method was then applied to detect numerous unknown oligomeric adducts. Therefore, the quantitative and qualitative transitions were used to verify that the detected 2D fingerprints did in fact originate from the same type of compounds as

the model compounds. With each PA–Mv adduct group, the ratios of the quantitative and qualitative transitions were determined using a single model compound for each adduct group, which were the main dimeric adducts with glucose moieties. The ratios were estimated as 99% confidence intervals. The confidence intervals were then further used to calculate how the qualitative fingerprints should look like based on the detected quantitative fingerprints (Figure 9). Finally, the measured qualitative fingerprints were compared to the predicted ones. The measured qualitative

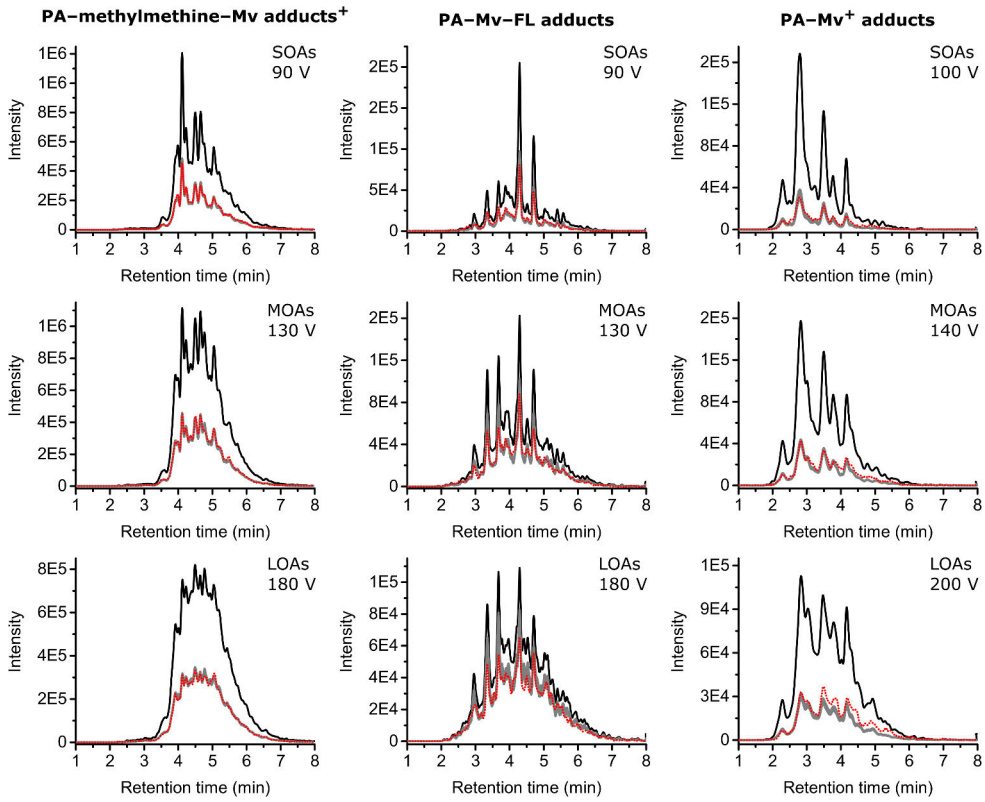

Figure 9. Validation of specificity of the detection of the PA–Mv adducts. The black lines represent the fingerprints acquired with the quantitative MRM transitions, and the red dotted lines represent the measured qualitative fingerprints. The grey areas were calculated based on the 99% confidence intervals for the ratios between the quantitative and qualitative transitions, which were determined with a single dimeric model compound of each compound group. In other words, they grey areas represent the approximate shape and location of the expected qualitative fingerprints. The numerical values in the top right corner in each panel are the cone voltages that were utilized in the MRM method in detection of the fingerprints. This figure was adapted from Article I with the permission of the copyright holder. Abbreviations: FL, flavan-3-ol monomer; LOAs, large oligomeric adducts; MOAs, medium-sized oligomeric adducts; Mv, malvidin glycoside; PA, proanthocyanidin; SOAs, small oligomeric adducts.

fingerprints matched the expected ones well, even though the ratios of the quantitative and qualitative MRM transitions were only estimated with a single model compound for each compound group, and only in one concentration. This meant that the methods were detecting the type of compounds that they were supposed to. Here, the validation of specificity is only presented with one example, but as can be seen later (chapter 3.2.1), the 2D fingerprints the oligomeric adducts were remarkably similar between multiple common wine types meaning that the validation results regarding specificity are generalizable.

Other crucial aspect to investigate and validate was the calibration of the methods. Ideally, a suitable quantification standard would have been a mixture that qualitatively resembled the actual wines but with known concentrations of the oligomeric PA–Mv adducts. Such standard was not available for calibration, and preparing such standard either by synthesis or fractionation has not been achieved thus far in the literature. Some calibration curves could have been prepared by using dimeric adducts as standards but, even then, there would have been considerable risk for inaccurate and misleading results, especially regarding the higher oligomers. That is because the efficiency of ionization and transformation of ions from liquid to gas phase can vary substantially in ESI even between relatively similar compounds (Gross, 2017a; Kebarle, 2000). Therefore, the calibration was performed by constructing calibration curves from a single reference wine, and the concentrations were reported as percentages of the unknown concentrations in the reference. The main reason for this approach was to account for the non-linear responses in many compound groups without having to dilute the wines. This approach enabled direct comparison of relative concentrations between wine samples. Importantly, this approach also enabled statistical modelling because the true concentrations in the analyzed red wines could have been obtained with a linear transformation, if the concentrations in the reference wine had been known. Calibration curves are presented as supplementary material in Article I. The method did not suffer from carryover and the intra-run repeatability was under 5% with most compound groups.

3.1.3 Summarizing the qualitative data of the 2D fingerprints

The group-specific method provided visual data about the compound composition in the form of 2D chromatographic fingerprints. A new tool was developed in Article III to simultaneously visualize and summarize this data from multiple samples to ease the recognition of compositional and evolutionary patterns. The comparison of individual 2D fingerprints between wine samples would have been inefficient, and it would have been difficult to establish generalizable patterns and to make solid conclusions. In general, it would not be acceptable to generalize a single measured concentration of some compound in one analyzed sample to concern the wider

population from which the sample was collected. Rather, multiple samples should be collected and analyzed, and an average result or other similar metric should be reported. Similar requirements should concern qualitative data as well, which was one reason for developing the visualization method. Briefly, the 2D fingerprints from multiple samples were combined and presented as 2D quantile fingerprints (Figures 10 and 12). This made it possible to condense chromatographic information from dozens of samples and hundreds of chromatograms into only a few quantile fingerprints. The solid black lines in the quantile fingerprints represent the median, and the grey regions are the ranges between 10^{th} and 90^{th} percentiles, i.e., where the individual fingerprints were the middle 80% of time. Practically, the grey areas in the quantile fingerprints represent within-group variation between the individual fingerprints. Refer to Article III for further discussion and for full step-by-step description of the method together with a visual example.

3.2 Composition of the oligomeric adducts in red wine

3.2.1 Composition in young red wines

The composition of oligomeric PA–Mv adducts were studied in young red wines (age 1–2 years) in Article III. Besides the age, the wine set was further limited by selecting only wines with at least 8 replicates based on the principal grape variety used in the wine making (n=92). These wines were the Pinot Noir, Shiraz, Merlot, Cabernet Sauvignon and Touriga Nacional wines. Most of these wines were single varietal wines besides the Touriga Nacional wines, all of which contained Touriga Franca and Tinta Roriz as secondary grapes. The Pinot Noir wines were further divided based on their region of origin, which were Beaune (France) and Pfalz (Germany).

The concentrations of the PA–Mv^+ adducts varied the most between wine types when compared to the other two groups of PA–Mv adducts. There was nearly a five-fold difference between the highest average concentrations (Cabernet Sauvignon, Shiraz and Touriga Nacional wines) and lowest average concentrations (Pinot Noir wines from the Beaune region) of the PA–Mv^+ adducts. The PA–Mv–FL adducts, on the other hand, had most variation in the SOA-%, MOA-% and LOA-% parameters between wine types, which indicated that these adducts had the most variation in average sizes of the adducts (Article III). Based on these size-distribution parameters, the Shiraz and Touriga Nacional wines had the highest average size of the PA–Mv–FL adducts, followed by the Merlot and Cabernet Sauvignon wines. The Pinot Noir wines had the lowest average size of the PA–Mv–FL adducts. The size-distribution parameters of the PA–Mv^+ and PA–methylmethine–Mv^+ adducts

suggested that the average size of the adducts was similar within the compound groups between all other wine types except the Pinot Noir wines from the Pfalz region. Without further calibration, the size-distribution parameters cannot reveal information about absolute differences in the average sizes of the adducts, but relative differences could still be established between wine types. Absolute concentrations could not be produced either, but accurate relative differences in concentrations were discovered between the wine types. Only few results regarding the concentrations and size-distribution parameters of the PA–Mv adducts in young wines are presented here as examples, and the detailed discussion can be found in Article III.

2D quantile fingerprints were calculated for the oligomeric adducts in the young red wines (Figure 10). Ten wines were randomly sampled for the 2D quantile fingerprints from Pinot Noir wines from the Pfalz region, and from the Merlot, Shiraz, and Cabernet Sauvignon wines. Additionally, all eight Pinot Noir wines from the Beaune region and all eight Touriga Nacional wines were used. The quantile fingerprints of three wine groups are presented in Figure 10 as examples, and the original figure in Article III presents the 2D quantile fingerprints from above-mentioned six wine groups. The fingerprints in Figure 10 revealed that the Pinot Noir wines differed significantly from the other two wine groups. This was likely linked to the fact that Pinot Noir wines only contain glucosidic anthocyanins and not acetylglucosidic and coumaroylglucosidic anthocyanins (Dimitrovska et al., 2011). Besides the Pinot Noir wines, the compositions of the other wine types resembled closely one another (Figure 10B and 10C; Article III). Only small differences in abundances of individual compounds were observed between the 2D fingerprints of the Merlot and Shiraz wines, but the chromatographic hump of the PA–Mv–FL adducts in the Shiraz wines was more prevalent than in the Merlot wines (Figure 10). This could be related to the implication of the size-distribution parameters, which suggested that the average size of the PA–Mv–FL adducts was higher in the Shiraz than in the Merlot wines, as mentioned earlier. Additionally, the within-group variation was negligible with the PA–Mv^+ adducts meaning that the individual wines were compositionally close to one another. However, there was more within-group variation in certain wine groups with the PA–methylmethine–Mv^+ adducts (Pinot Noir wines from Beaune region and Merlot wines) and the PA–Mv–FL adducts (Merlot wines). The general outcome about the composition of the oligomeric adducts in young red wines in Article III was that the quantitative differences between wine types were more substantial than qualitative compositional differences. As a note, the PA content in commercial red wines was studied in Article IV and the main outcome was similar; based on the 2D quantile fingerprints and the quantification results of PAs, the quantitative differences appeared to be more substantial between wine types than the qualitative differences.

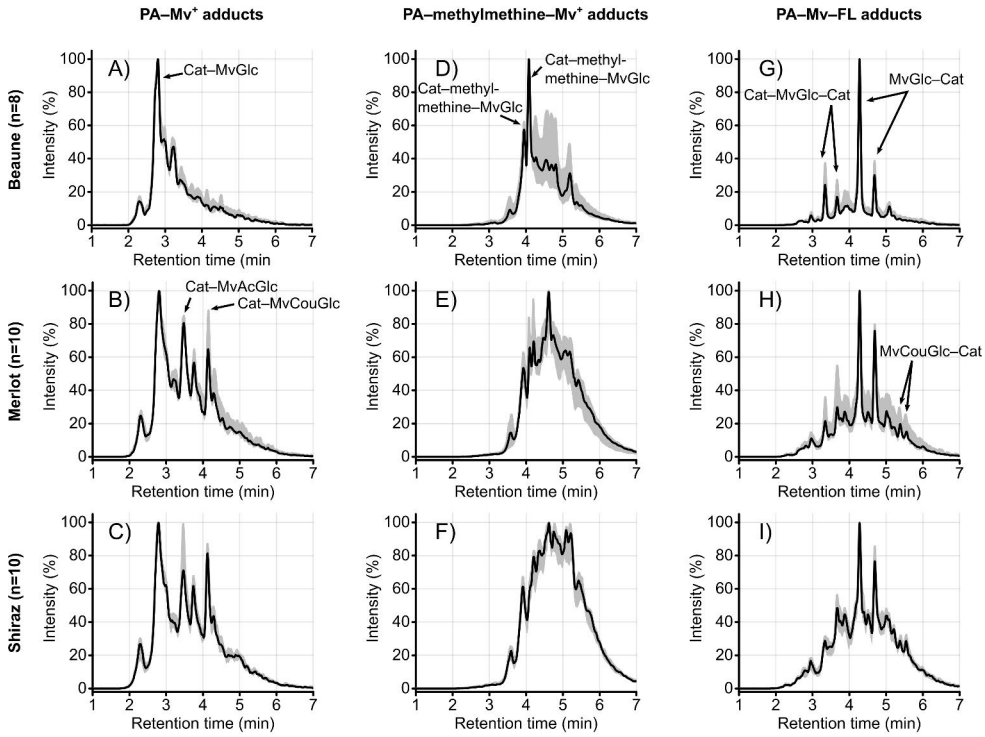

Figure 10. Two-dimensional (2D) quantile fingerprints of the proanthocyanidin–malvidin glycoside adducts in young (1–2 years) Pinot Noir wines from the Beaune region (A, D, G), Merlot wines (B, E, H) and Shiraz wines (C, F, I). The black lines represent median fingerprints, and the grey areas represent the interval between 10th and 90th percentiles, i.e., the grey areas represent the within-group variation. Overall, 28 wines were sampled for this figure, there were three compound groups, and each group was detected separately as small, medium-sized and large oligomeric adducts, meaning that chromatographic information from 252 individual fingerprints were condensed into these 9 quantile fingerprints. The figure was adapted from Article III with the permission of the copyright holder. Refer to the original figure in Article III for similar plots of three additional wine types. Refer to Article I for the characterization of the individual compounds. Abbreviations: Cat, catechin; FL, flavan-3-ol monomer; Mv, malvidin glycoside; MvAcGlc, malvidin-3-*O*-acetylglucoside; MvCouGlc, malvidin-3-*O*-coumaroylglucoside; MvGlc, malvidin-3-*O*-glucoside; PA, proanthocyanidin.

3.2.2 Evolution of the oligomeric adducts

The evolution of the oligomeric adducts was studied by grouping red wines by their age (Article III). Only wines that contained Merlot, Shiraz or Cabernet Sauvignon grapes as the primary grapes were used for this purpose because they had similar qualitative and quantitative compositions in the young wines. In total, 95 wines were selected to this subset of wines, and it was possible to recreate known evolutionary trends of the monomeric pigments with the subset. For instance, a strong decrease in the concentration of malvidin glycosides and B-type vitisins was observed, and the pinotin-type malvidin derivates were found to be relatively stable (data not shown). These trends have been reported in literature before for red wines during bottled storage (Arapitsas et al., 2012; Boido et al., 2006; Zhang et al., 2021). Overall, these results validated the suitability of the selected sub-set for this study.

Evolution of the concentrations and average sizes of the adducts

The PA–Mv–FL adducts were the most stable of the three groups of oligomeric adducts, and the stability concerned both the concentrations and the size-distribution parameters (Figure 11C and F). The size-distribution parameters indicated that the average sizes of the PA–Mv–FL adducts did not change significantly towards older wines. A decreasing trend in the concentrations was observed with the PA–Mv^+ adducts (Figure 11A). Moreover, the SOA-% and MOA-% decreased while the LOA-% increased towards older wines, which suggested that there was an evolutionary trend in the average sizes of the adducts (Figure 11D). More specifically, the average size of the adducts appeared to increase towards the older wines. However, the PA–methylmethine–Mv^+ adducts were clearly the least stable compound group as a significant decreasing evolutionary trend was established in the concentrations (Figure 11B). Importantly, the SOA-% and MOA-% decreased strongly as well, while the LOA-% increased correspondingly (Figure 11D). This suggested that while the concentrations of the PA–methylmethine–Mv^+ decreased significantly towards the older wines, the average size of the remaining adducts was higher in the old wines than in the young wines.

Similar studies about evolutionary trends have been performed before by measuring concentrations of individual oligomers in red wine (Alcalde-Eon et al., 2006; Arapitsas et al., 2012; Blanco-Vega et al., 2014; Boido et al., 2006; Zhang et al., 2021). In these cases, the measured oligomers were mainly dimers, and the evolutionary trends of the whole compound groups had to be estimated based on the evolutionary trends of the dimers. However, the evolutionary trends of the dimers might not necessarily reflect the trends of the higher oligomers. Now, a more comprehensive selection of compounds was measured with the group-specific method, which meant that no such generalization was needed because of the novel

methodology. With that said, the quantitative evolutionary trends that were established in the literature based on the dimeric adducts matched those reported in Article III for the whole compound groups. Namely, the concentrations of dimers belonging to the PA–methylmethine–Mv^+ adduct group have been shown to decrease rapidly during bottled storage, and the concentrations of dimers belonging to the PA–Mv^+ adduct group decrease as well, but much slower (Arapitsas et al., 2012; Boido et al., 2006; Zhang et al., 2021). There is only little literature data about the evolution of the PA–Mv–FL adducts, but in one study the concentration of a dimer of this group was shown to decrease slowly towards older red wines (Zhang et al., 2021). Importantly, the size-distribution parameters provided completely new insight into the evolution of the average sizes of the adducts. Similar information cannot be achieved by monitoring only the individual small oligomers. Therefore, to literature comparison could be done, because this was the first time that evolutionary data of this sort was reported at compound group level.

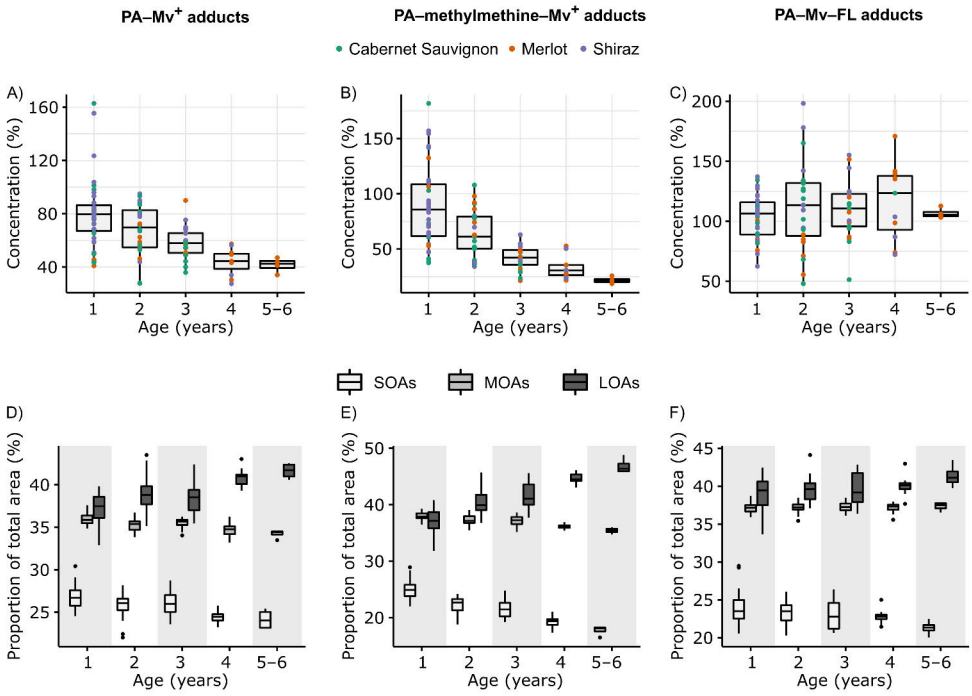

Figure 11. Evolution of the concentrations (A–C) and size-distribution parameters (D–F) of the proanthocyanidin–malvidin glycoside adducts in red wines. The evolution of the adducts was studied with red wines where the primary grape variety was either Cabernet Sauvignon, Merlot or Shiraz (n=95). Most wines were single-varietal wines. This figure was adapted from Article III with the permission of the copyright holder. Abbreviations: FL, flavan-3-ol monomer; LOAs, large oligomeric adducts; MOAs, medium-sized oligomeric adducts; Mv, malvidin glycoside; PA, proanthocyanidin; SOAs, small oligomeric adducts.

Evolution of the 2D chromatographic fingerprints

Besides the size-distribution parameters, the 2D fingerprints offered a new way to assess the evolution of the oligomeric adducts (Figure 12). Generally, the evolutionary trends were modest, but they were still established with high certainty because of the utilized visualization tool that combined information from dozens of red wines. With the PA–Mv^+ adducts, the abundance of the individual dimers decreased, and the underlying chromatographic hump became more pronounced towards older wines, although the differences were minor (Figure 12A–12C). This

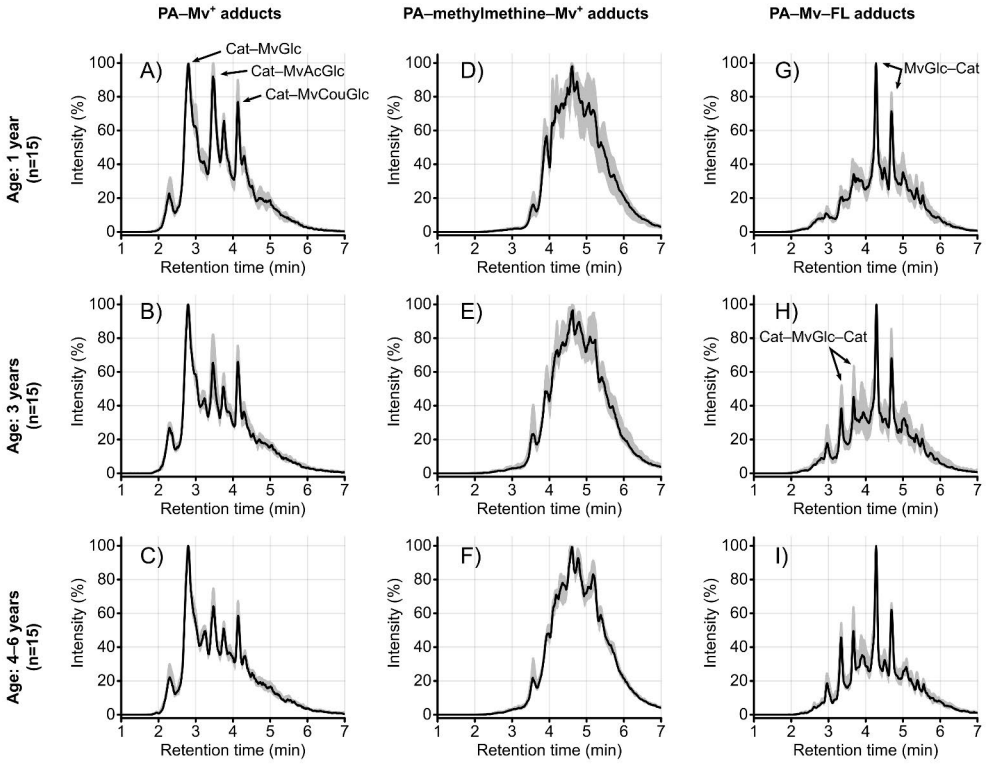

Figure 12. Two-dimensional (2D) quantile fingerprints of the proanthocyanidin-malvidin glycoside adducts in Shiraz, Merlot, and Cabernet Sauvignon wines of different ages. The black lines represent median fingerprints, and the grey areas represent the interval between 10th and 90th percentiles, i.e., the grey area represents within-group variation. Overall, 45 wines were sampled for this figure, there were three compound groups, and each group was detected separately as small, medium-sized and large oligomeric adducts, meaning that chromatographic information from 405 individual fingerprints were condensed into these 9 quantile fingerprints. The figure was adapted from Article III with permission of the copyright holder. Abbreviations: Cat, catechin; FL, flavan-3-ol monomer; Mv, malvidin glycoside; MvAcGlc, malvidin-3-*O*-acetylglucoside; MvCouGlc, malvidin-3-*O*-coumaroylglucoside; MvGlc, malvidin-3-*O*-glucoside; PA, proanthocyanidin.

observation was in-line with the conclusion made from the evolution of the size distribution parameters, which suggested that the average size of the adducts increased. The strongest trend in the 2D quantile fingerprints of the PA–methylmethine–Mv^+ adducts was that the within-group variation decreased significantly (Figure 12D–12F). In other words, there was variation in the composition of the adducts in the 1-year-old wines, but as the wines aged the compositions converged. Interestingly, the size-distribution parameters implied that the average sizes of the PA–methylmethine–Mv^+ adducts changed the most out of the three compound groups, but no clear visual changes could be seen in the 2D fingerprints. Evolutionary changes in the composition of the PA–methylmethine–Mv^+ adducts were likely hidden in the 2D fingerprints by the complexity of the compound group and the fingerprints themselves. There was no significant evolution in the average sizes of the PA–Mv–FL adducts based on the size-distribution parameters, but an evolutionary trend was seen in the 2D quantile fingerprints (Figure 12G–12I). Trimeric adducts of this compound group appeared in the 3-year-old wines and the middle point of the hump seemed to move to lower retention time.

3.2.3 Factors regulating formation of the oligomeric adducts

A subset consisting only of the 1-year-old wines was utilized to examine which factors could potentially influence the formation of oligomeric adducts (n=78, Article III). The concentrations and the LOA-% of the oligomeric adducts were modelled with the concentrations of PAs, FLs and Mvs, with the ratios of the concentrations of FLs and PAs (FL/PA), and with the mDP of PAs. The FL/PA ratio was used as a predictor because of the shared nucleophilic properties of PAs and FLs. This could cause competition between PAs and FLs in the formation of some oligomeric adduct groups, namely the PA–methylmethine–Mv^+ and PA–Mv–FL adducts. The LOA-% was the only size-distribution parameter that was modelled because the LOA-% correlated strongly and negatively with the SOA-%, and moderately and negatively with MOA-% in the whole wine set (n=317, Article II). Therefore, the LOA-% alone contained information about the proportions of the other two size-distribution parameters. The PLSR models for the PA–Mv^+ adducts are presented in Figure 13 as examples, and the models for the other two compound groups are presented in Article III. It is recognised that the experimental design was not optimal because the formation of the adducts was studied using commercial wines that were already 1-year-old. The experimental design relies on the assumption that the determined predictors in the 1-year-old wines reflect their initial values at the beginning of the wine making. Therefore, the following results should be considered as tentative results that could inspire further examinations.

73% of the PA–Mv^+ concentrations could be explained with the measured composition of starting materials (Figure 13). The Mv concentration was an important factor in the PLSR model while the PA concentration was not (Figure 13A), suggesting that the Mv concentration was a limiting factor in formation of the PA–Mv^+ adducts. Interestingly, the mDP of the PAs seemed to contribute to the formation of the PA–Mv^+ adducts significantly as well (Figure 13A). This could be explained by considering the formation mechanism of these adducts. The mechanism requires the formation of positively charged carbocationic degradation products from the extension units of PAs, which are formed by acid-catalyzed cleavage of the C–C bonds between constituting units (Salas et al., 2003). The number of C–C bonds between the constituting units increases as the mDP of PAs increases, which provides more possible sites for the formation of the carbocationic intermediates. The LOA-% of the PA–Mv^+ adducts was relatively well explained by the starting material composition as well (61% of variation explained; Figure 13B). The single most important factor was the FL/PA ratio, which had a negative regression coefficient, and the FL/PA ratio had stronger connection to the LOA-% than the concentrations of FLs and PAs as such. In other words, high PA content compared to FL content favoured the formation of larger adducts. The FL/PA ratio was an important predictor for the LOA-% with the other two PA–Mv adduct groups as well (Article II). One possible reason that concerns all three PA–Mv groups could be that high PA content favours the release of reactive carbocationic intermediates, and the simultaneously low FL content would mean that there are less FLs to compete with the oligomeric PA–Mv adducts in the repolymerization reactions.

The models for the other two adduct groups are discussed in detail in Article III. Briefly, 59% of the variation in the PA–methylmethine–Mv^+ concentrations were explained with the measured starting materials, but only 11% of the variation in the PA–Mv–FL concentrations could be explained by the PLSR model. Additionally, 80% of the variation in the LOA-% of PA–Mv–FL adducts and 63% of the LOA-% of the PA–methylmethine–Mv+ adducts were explained by the PLSR models. The analysis of these results is covered in Article III, where an explanation is given to the poor fit of the model describing the formation of the PA–Mv–FL adducts, for instance.

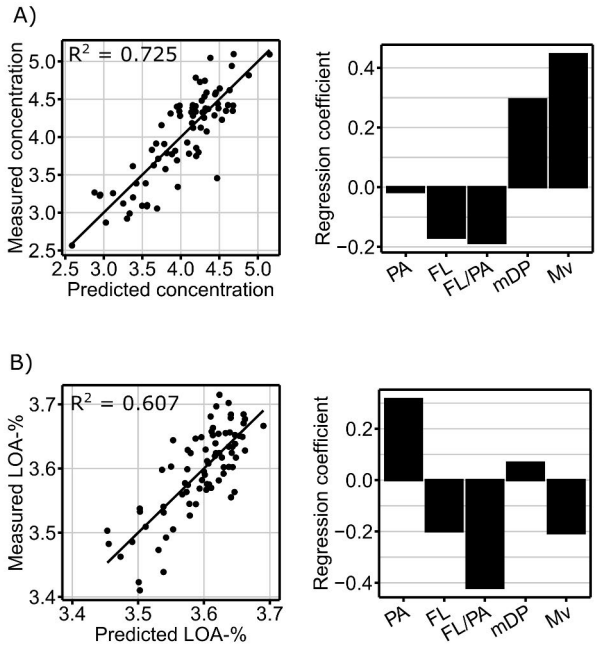

Figure 13. Partials least squared regression (PLSR) models explaining the concentrations (A) and proportions of large oligomeric adducts (LOA-%; B) of the PA–Mv^+ adducts in the 1-yeard-old wines (n=78). The concentrations of proanthocyanidins (PA), flavan-3-ol monomers (FL) and malvidin glycosides (Mv) were used as predictors, in addition to the mean degree of polymerization (mDP) of PAs and the ratio of the concentrations of the FLs and PAs (FL/PA). Both response variables were modelled with separate PLSR models. Refer to Article III for similar models for the PA–methylmethine–Mv^+ and PA–Mv–FL adducts. The figure was adapted from Article III with the permission of the copyright holder.

3.3 Sensorial properties of red wine

3.3.1 Colour intensity

Only smaller sub-sets of the whole wine set were utilized in chapters 3.1. and 3.2. However, it was possible to exploit all wines in the analysis of the wine colour in Article II because there was no need to categorize wines in any way, and the aim was to establish general connections between the expressed colour intensity and the content of the pigments. The three-component PLSR model explained 83% of the variation in the colour intensity in the 317 wines, i.e., most of the variation in the colour intensity could explained by the measured pigment composition (Figure 14).

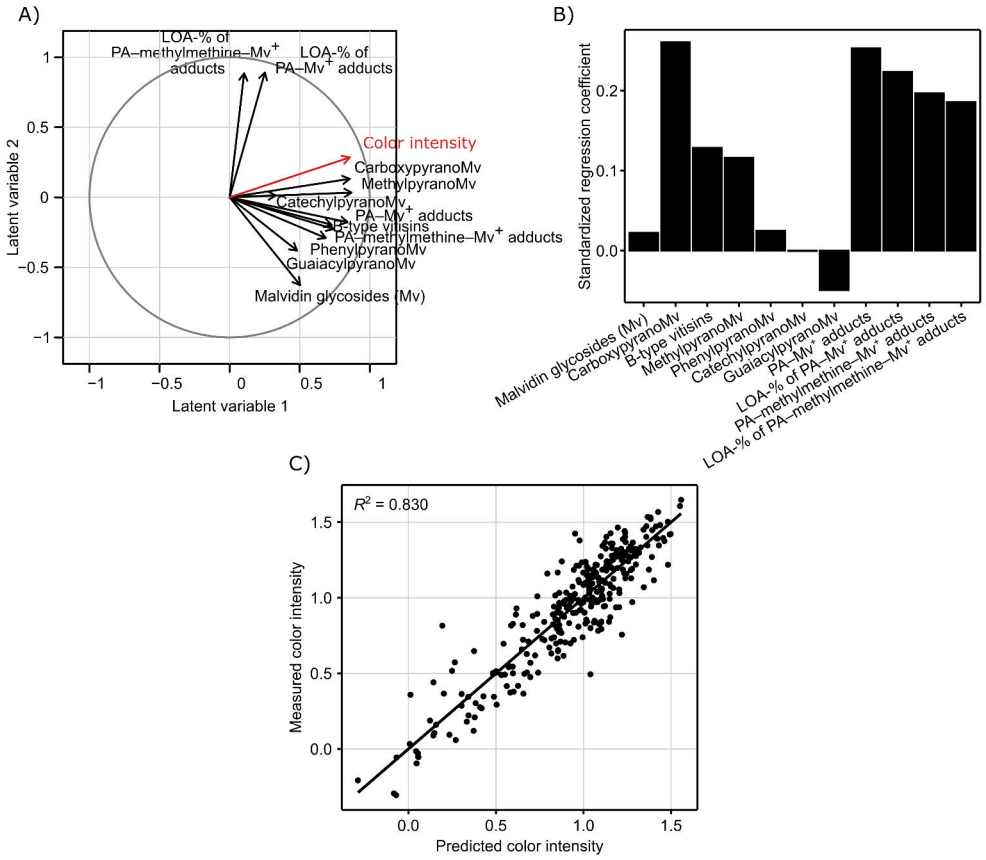

Figure 14. Results of the partial least squares regression (PLSR) model for the color intensity of the red wines (n=317). Panel A shows correlations between the response and predictor variables on the two first latent variables, panel B shows the standardized regression coefficients of the three-component model and panel C shows the scatter plot of the predicted and measured colour intensities. The greater the regression coefficient is in panel B, the more important is the variable for the PLSR model. This figure was adapted from Article II with permission of the copyright holder. Abbreviations: LOA-%, proportion of the large oligomeric adducts of the total response; Mv, malvidin glycoside; PA, proanthocyanidin.

The carboxypyranomalvidin glycosides, PA–Mv^+ adducts and PA–methylmethine–Mv^+ adducts were the most important compound groups in terms of the concentrations in explaining the colour intensity (Figures 14A and 14B). Importantly, the LOA-% of the PA–Mv^+ and PA–methylmethine–Mv^+ adducts were important predictors as well with positive connection to colour intensity. This suggested that an increase in the average sizes of the oligomeric adducts had a positive impact on the colour intensity of the wines. Moreover, the LOA-% of the two oligomeric adduct groups explained such portion of the variation in the colour intensity that could not be explained by the concentrations of the pigments (Figure

14A). This could be concluded because the second latent variable, which explained 8.1% of the variation in the colour intensity, was mainly described by the LOA-% variables (Figure 14A). One possible reasoning for this result could be that the colour properties of the oligomeric adducts are affected by intramolecular copigmentation, and its efficiency would be proportional to the length of the PA moieties in the adducts. Alternatively, the PA moieties could protect the chromophores from attacking nucleophiles such as H_2O, which would reduce the formation of the colourless hemiacetals. These mechanisms are further discussed in Article II. The methylpyranomalvidin glycosides and B-type vitisins had moderate connection to colour intensity in the PLSR model, while the concentrations of pinotin-type pigments and the malvidin glycosides did not have a significant impact on the colour intensity.

A second PLSR model for the colour intensity was fitted using only the 1-year-old wines and the results are presented in Article II. The biggest differences compared to the model with all wines was that B-type vitisins were more impactful on the colour intensity, and the LOA-% of the PA–methylmethine–Mv^+ adducts was not a significant feature. The pinotin-type pigments still had only minor or no connection to measured colour intensity, and the malvidin glycosides were more impactful on the colour intensity, but their contribution remained only moderate. Implications of these results are discussed in detail in Article II.

This is the first time that the contributions of two specific groups of oligomeric PA–Mv adducts to the colour intensity were studied at compound group level. Previous studies have either focused on the individual dimers and their properties in isolated conditions, or to correlations between colour properties and individual small oligomers (Boido et al., 2006; Dueñas et al., 2006; Nave et al., 2010; Oliveira et al., 2013). Here, the pigments were studied in their true complex environments, i.e., in red wines, and a more complete picture of the PA–Mv adduct composition was used in modelling the colour intensity than is typical in the literature.

3.3.2 Sensorially evaluated tannicity

The sensorially perceived tannin content, i.e., tannicity was estimated from 201 red wines at Alko Inc. (Article IV). Astringency can be defined as the complex of sensations due to shrinking, drawing or puckering of the epithelium as a result of exposure to substances such as alums or tannins (García-Estévez et al., 2018). This definition describes similar types of sensations as the definition of tannicity given in material and methods (chapter 2.6.3.). Therefore, the results obtained herein about tannicity should provide information about astringency as well. The discriminant-type evaluations were done at Alko Inc. primarily to support their own sales personnel, and to provide information about the red wines to the customers of Alko

Inc. Similar sensorial analyzes are routinely performed at Alko Inc, and Alko Inc. lists the tannicity evaluations in their web page at www.alko.fi for most red wines in their selection. Even though the sensorial analyzes were not primarily conducted to produce research data, the results could be utilized for research purposes when combined with chemical and statistical analysis. The methodology might be unconventional in sensorial analysis, and there were fewer panelists evaluating each wine than is typical, for instance. However, the strength of the utilized sensorial data set was in its size. Just over 200 red wines were evaluated by few dozen panelists in total, meaning that the large data set was well suited for statistical analysis. It was assumed that the wines were evaluated correctly on average despite each wine being evaluated by low number of panelists, which would mean that the conclusions made from the statistical model should be valid on average as well. Should a trend be discovered in a thoroughly cross-validated statistical model containing over 200 wines, it would be a strong indicator on what chemical traits might drive the sensation of tannicity.

Overall, the three-component PLS-DA model achieved an average error rate of 18.8% in cross-validation, and 17.4% for the whole wine set, i.e., fewer than every fifth wine was incorrectly classified. The low error rates indicated that the classification of the wines was not random, and that the sensorially evaluated tannin content was explained relatively accurately by the measured chemical composition. The variables that were the most strongly associated with the tannic wines, i.e., the tannicity group with more tannins, were the LOA-% of the PA–Mv^+, PA–Mv–FL and PA–methylmethine–Mv^+ adducts, and the mDP and PD-% of PAs (Figure 15B). These same variables were also the most important variables in the statistical model overall (Figure 15C). The concentrations of the PAs and PA–Mv adducts, on the other hand, were less important in explaining the perceived tannicity.

The result that the PA concentration was not a major contributor to tannicity was not unique. Other studies have shown before that the total PA or tannin concentration is not necessarily correlated with astringency-related sensations (Quijada-Morín et al., 2012; Watrelot et al., 2016). One reason explaining the lack of significancy of the PA concentration could be that the concentration of PAs was high enough in all wines, so that any increase in it could no further increase the sensation of tannicity. The tested concentration range of PAs was also given as explanation for the lack of statistical significance between the PA concentration and astringency by Quijada-Morín et al. (2012). The average sizes of the PAs and PA adducts impacted the sensation of tannicity significantly (Figure 15B and C). The degree of oligomerization of PAs is generally regarded as one of the driving factors for astringency, and this result was recreated in the present study, which validated the utilized methodology (Chira et al., 2012; Freitas & Mateus, 2002; García-Estévez et al., 2018; Vidal et al., 2004). However, the average sizes of specific groups of PA–

Mv adducts have not been experimentally shown to contribute to tannicity or to astringency before.

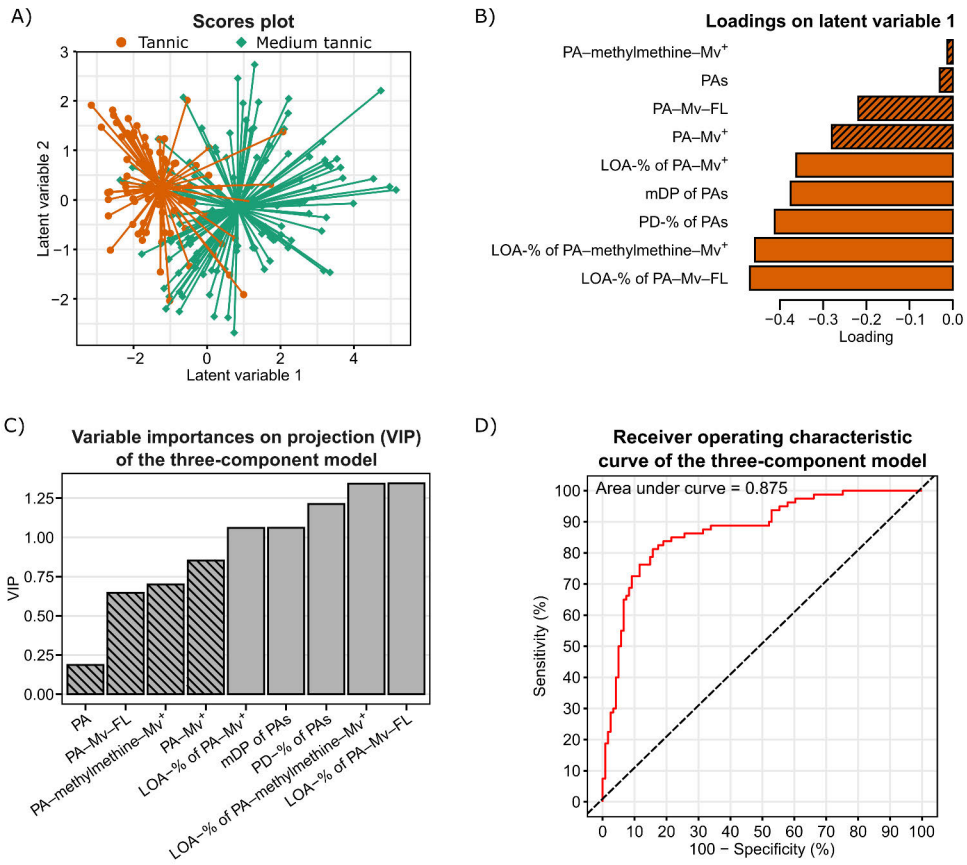

Figure 15. Results of the partial least squares discriminant analysis (PLS-DA) explaining the sensorially evaluated tannicity with the compositions of proanthocyanidins (PA) and proanthocyanidin–malvidin glycoside adducts (PA–Mv). Panel A shows the scores plot of the wines (n=201) on the first two latent variables, and panel B shows the loadings of the variables on the first latent variable. Panel C shows variable importance on projection (VIP) of the three-component model, and panel D shows the receiver operating characteristics plot of the three-component model. The rasterized bars in panels B and C indicate variables related to concentrations, and the non-rasterized bars indicate variables related to composition of the compound groups. Abbreviations: FL, flavan-3-ol monomer; LOA-%, proportion of the large-oligomeric adducts of the total response; mDP, mean degree of polymerization; Mv, malvidin glycoside PA, proanthocyanidin; PD-%, proportion of prodelphinidin units in the PAs; VIP, variable importance on projection.

The polymeric pigments have been shown to have contribution to astringency, but in these cases the analytical methods were relatively universal for polymeric pigments in general, and not for any specific sub-group (Gawel et al., 2007; Ristic et al., 2010). Therefore, this was the first time that specific groups of PA–Mv adducts were shown to be associated with mouth-feel of red wines at a compound group level. Due to the limitations in the methodology of the sensorial analyzes, the present results should still be considered as tentative.

3.4 Synthesis and properties of procyanidin analogs

The aldehyde-mediated PC analogs were expected to differ in their chemical and biological properties in comparison to natural PC oligomers for few different reasons. First, the methine or substituted methylene groups that connect the catechin units should provide more structural flexibility to the PC analogs compared to the direct linkages between the constituting units in the natural PC oligomers. Regarding the PPC, both the structural flexibility and three-dimensional structure of tannins are known to affect the PPC (Cala et al., 2010; Quideau et al., 2011). Moreover, the aldehydes used in the hemisyntheses could be chosen so that they introduce certain moieties to the linkage units of the PC analogs that could actively participate to the protein interactions, namely catechol and pyrogallol groups. These two groups are found in PAs as the B-rings of PCs and PDs, respectively. The B-rings are known to be the structural moieties in catechins and gallocatechins that have the closest interaction with BSA based on NMR experiments (Xu et al., 2009). Similarly, the B-rings of PC dimer B2 have stronger interaction with BSA than other parts of the molecule based on NMR experiments as well (Soares et al., 2018). Specific structural moieties of PCs cannot always be identified as the primary binding sites with proteins, as was observed in interaction between PC trimer C1 and BSA, and in interactions between PC dimers B1–B4 and proline-rich proteins (Cala et al., 2010; Soares et al., 2018). However, the catechol groups, and presumably pyrogallol groups, can certainly participate in the protein interactions in PAs. The octanol-water partition and stability in PBS were determined in addition to the PPC to gain better understanding about the properties of the PC analogs, and the linkage units were expected to affect these properties as well.

Ten dimeric PC analogs were synthesized in total from catechin or epicatechin and five different aldehydes (Figure 5). The utilized hemisynthesis strategy was based on the common concept utilized in many synthesis experiments and studies with model wine solutions, but the exact conditions (e.g., solvent, volume, and concentrations) were optimized specifically for this study to enable rapid synthesis and purification of the PC analogs (Es-Safi, Cheynier, et al., 2000; Nonier Bourden

et al., 2008; Pissarra et al., 2003). The chosen aldehydes were formaldehyde, glyoxylic acid, furfural, 3,4-DBA and 3,4,5-TBA. Formaldehyde was chosen to introduce the simplest possible linker unit to the PC analogs, i.e, a methylene group. Furfural and glyoxylic acid are known to be reactive aldehydes with catechins based on literature, and especially the glyoxylic acid is known the react with catechin with good yields (Es-Safi, Cheynier, et al., 2000; Es-Safi, Le Guernevé, et al., 2000; Nonier Bourden et al., 2008). The 3,4-DBA and 3,4,5-TBA were chosen to introduce catecholmethine and pyrogalloylmethine linkers to the PC analogs. Formaldehyde, furfural, and glyoxylic acid have been used in the aldehyde-mediated synthesis of FL dimers, or FL and Mv dimers before (Drinkine et al., 2005; Es-Safi, Cheynier, et al., 2000; Nonier Bourden et al., 2008; Pissarra et al., 2003). However, the dimers obtained from reactions between (epi)catechins and 3,4-DBA or 3,4,5-TBA were novel.

The yields of the isolated PC analogs were 3–18% and each product was characterized based on their high-resolution mass spectra and the calculated molecular formulae, UV–Vis spectra and NMR spectra. Briefly, the molecular formulae calculated from the mass spectra matched the expected products, and the UV–Vis spectra were nearly identical to catechin and epicatechin, which was expected for the products as well. The intramolecular linkage between the catechin or epicatechin units can be either at C6 or C8 position in both units. Literature data from corresponding reactions shows that the main dimeric products are always C8–C8 linked, and this could be confirmed for most of the synthesized PC analogs as well (Drinkine et al., 2005; Escribano-Bailón et al., 1996; Fulcrand et al., 1997; Lee et al., 2004; Pissarra et al., 2005; Shoji et al., 2002). Eight out of the ten PC analogs could be verified to be C8–C8 linked based on their HMBC NMR spectra. Briefly, the hydrogen in the methylene or methine groups between the catechin units was observed to correlate with the C8a carbons of the catechins, which was only possible if the linkage was at C8–C8 position. The linkage position of two compounds could not be conclusively verified, and these compounds were the catechin-based dimers with catecholmethine and pyrogallolmethine linkers. However, the corresponding dimers synthesized from epicatechin were confirmed to be C8–C8 linked, as were the other six PC analogs as well. Considering the literature data about similar reactions (cited above), and the similarity of the NMR spectra between all PC analogs, the catechin-based dimers with catecholmethine and pyrogallolmethine linked PC analogs were presumed to be C8–C8 linked as well. The characterization is covered in greater detail in Article V.

3.4.1 Protein precipitation capacity

All PC analogs had substantially improved PPC in comparison to the PC dimers B2 and B3, while the PPC of PC trimer C1 and EGCG were still superior to all dimers (Figure 16). The PC dimers B2 and B3 did not have practically any activity in the conducted experiment. However, even the PC analog with a methylene-linker did exhibit significantly improved PPC compared to the PC dimers B2 and B3, which meant that the more flexible linkage alone increased the PPC substantially. The PC analogs with carboxymethine-linkers had only marginally improved PPC compared to the PC analog with methylene-linker. The PPC was further improved with the PC analogs with furanmethine, catecholmethine and pyrogallolmethine linkers. One potential explanation for the increased activity could be the active participation of these structural moieties to the interactions with the BSA. Non-specific interactions between proteins and PAs are generally presumed to happen via hydrogen bonding, π-π stacking or hydrophobic interactions, and these mechanisms should be viable for the furanmethine, catecholmethine and pyrogallolmethine groups in the PC analogs (Mcrae & Kennedy, 2011; Quideau et al., 2011). More detailed discussion and further results are presented in Article V. The PPC results have natural implications for red wine as well, as PPC of PAs is linked to the astringency of red wine, even though astringency was not the main motivator for the PPC experiment.

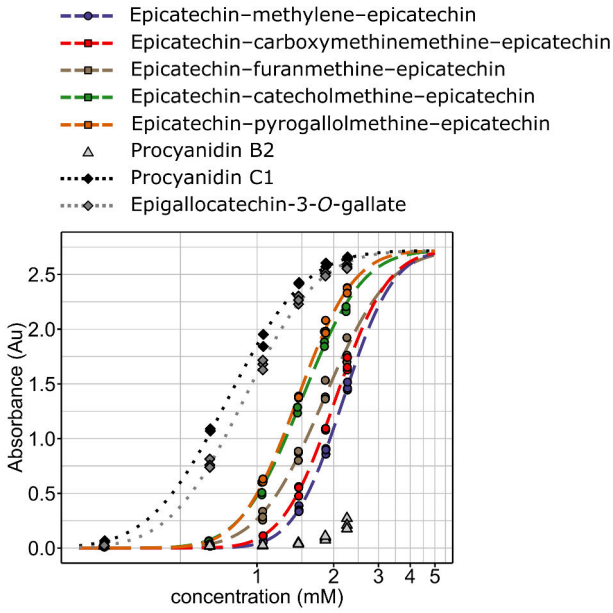

Figure 16. Fitted curves of the log-normal dose–response model for the protein precipitation capacity of the epicatechin-based PC analogs, and the reference compounds. Refer to Article V for similar figure of the catechin-based PC analogs.

3.4.2 Octanol-water partition

The linkage unit in the PC analogs had a substantial impact on the octanol–water partition. The log*P* varied between −1.78 (epicatechin–carboxymethine–epicatechin) and 0.72 (catechin–furanmethine–catechin) meaning that some PC analogs were hydrophobic and some hydrophilic. For reference, the PC oligomers B2, B3 and C1 were always hydrophilic with negative log*P* values (−0.87, −0.79 and −1.17, respectively), whereas catechin and epicatechin were hydrophobic with positive log*P* values (0.42 and 0.16, respectively). The variation in the log*P* values was an interesting discovery because it meant that the hydrophobicity of the PC analogs can be adjusted by the selection of the linkage unit, depending on what kind of property is desired. Importantly, the log*P* did not correlate with the PPC within the studied set of compounds.

3.4.3 Stability in phosphate buffered saline

Stability was the third key property determined for the PC analogs and the reference compounds. Stability in PBS was of interest because PBS is commonly used matrix in biological research (Cao et al., 2020). Moreover, flavonoids with catechol and especially pyrogallol groups are known to be unstable in neutral PBS buffers (Cao et al., 2020; Hatano et al., 2003). Other bioactive polyphenols, such as hydrolysable tannins are also unstable in such conditions (Baert, 2017; Engström et al., 2016). The synthetic PC analogs were more unstable than the corresponding PC oligomers B2 ($t_{1/2}$ 693 min), B3 ($t_{1/2}$ 539 min) and C1 ($t_{1/2}$ 1852 min). The most unstable compounds were the synthetic PC analogs with pyrogallolmethine linkers, which were so unstable that no analyte was present even at the first measured time point. EGCG ($t_{1/2}$ 84 min), which also contains pyrogallol groups, was amongst the most unstable compounds as well. The half-lives of the PC analogs with catecholmethine linkers ($t_{1/2}$ 55 and 84 min) were comparable to the half-life of EGCG. The most stable PC analogs were the ones with carboxymethine ($t_{1/2}$ 376 and 420 min) and furanmethine linkers ($t_{1/2}$ 531 and 349 min). Kinetic curves and compound-specific half-lives are presented in Article V with further discussion.

Interestingly, different kinds of degradation products were observed to form from different PC analogs, even though the PC analogs only differed in their linking units (Figure 17; Article V). The chromatograms of the reaction mixtures of two PC analogs are given in Figure 17 as an example, while the rest of data is presented in Article V. The stability of the tested compounds was not always correlated with the complexity of the formed reaction mixtures. For instance, the carboxymethine-linked PC analogs were relatively stable amongst the PC analogs. Yet, they still formed several different types of oxidation products with molecular formulae such as $M-H_2$, $M+O_2$ and $M-H_4O$, and multiple uncharacterized products were formed

in smaller proportions as well (Figure 17A). In this notation, the symbol M represents the molecular formula of the discussed compound, and the rest of the notation implies to the changes in the formula. The catecholmethine-linked PC analogs were more unstable than the carboxymethine-linked PC analogs, but only products $M-H_2$ and $M-H_4$ were formed in significant quantities with the latter being the main products (Figure 17B). The most complex mixtures of products were formed from the pyrogallolmethine-linked PC analogs and EGCG, which was likely related to the pyrogallol moieties. These compounds formed dimeric products, and EGCG is indeed known to dimerize in PBS solution via *o*-quinone intermediates (Hatano et al., 2004; Tanaka et al., 2002). Although (epi)catechin was relatively stable in the tested PBS solution, they were observed to form highly oligomerized and oxidized products up to nonamers.

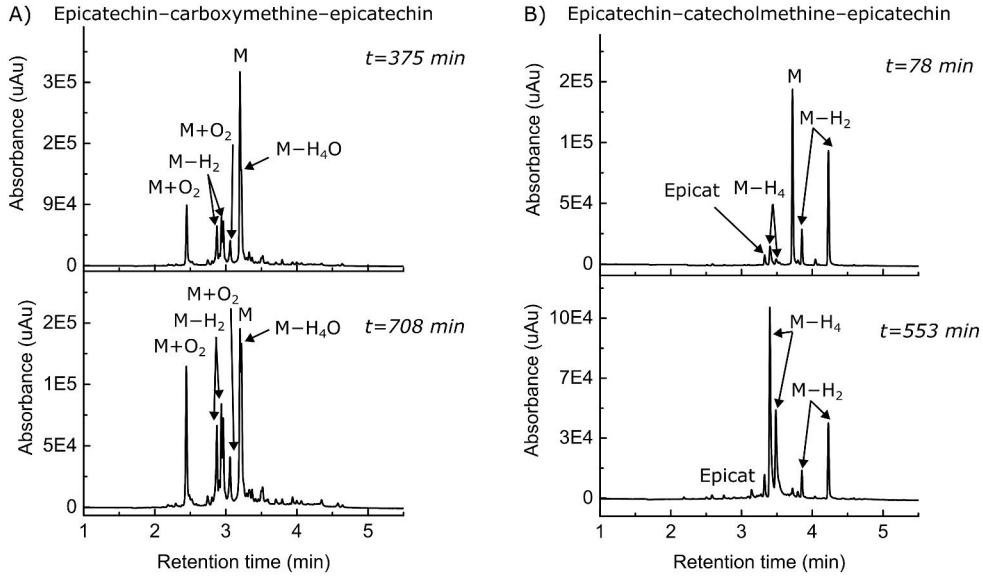

Figure 17. UV chromatograms (280 nm) of two epicatechin-based PC analogs from the stability experiments. Upper chromatograms are at the half-lives of the two compounds and the bottoms ones either at the end of the experiment (A), or at the time point when all starting material had been consumed (B). The letter M stands for the molecular formula of the tested compound and the rest of the notation implies to the changes in the formula in the products. Refer to Article V for similar chromatograms of the other tested compounds and for the full compound characterization data.

The $M-H_2$ products of the PC analogs most likely corresponded to formation of new intramolecular linkages between the constituting units, or between the linkage units and one of the constituting units. One possible mechanism for formation of the new linkages is the mechanism leading to formation of dehydrocatechins from

catechins (Sun & Miller, 2003). In this mechanism, a B-ring of one catechin molecule oxidizes to yield an electrophilic *o*-quinone structure, which is then attacked by the nucleophilic C6 or C8 carbons of the A-ring of another catechin molecule. Although many compounds exhibited similar changes in molecular formulae, the formed products were not necessarily similar in all cases because the UV spectra differed between various $M-H_2$ products. The UV spectra of the initial PC analogs themselves, however, were always nearly identical between one another, and with catechin and epicatechin as well. Some of the products, such as $M-H_4O$ products of the carboxymethine-linked dimers and the dimers of EGCG could be identified based on earlier literature, but most compounds could be only tentatively identified (Es-Safi, Le Guernevé, et al., 1999; Hatano et al., 2003). More detailed discussion and further results of the stability experiments can be found in Article V.

4 Conclusions

Red wine is an exemplary matrix in demonstrating the chemical reactivity of PAs and anthocyanins, and the chemistry of red wine can be used as inspiration for other studies in wholly another context. The biological properties of PAs and other natural compounds have always been one of the main areas of focus in chemistry of natural products. The analytical work with red wines led to an idea on how the reactivity of PAs and FLs could be utilized to contribute to this field of chemistry as well, and the author wished to pursue the idea. Indeed, the properties of the hemisynthesized PC analogs were improved or altered in comparison to natural PC dimers. The PPC of the dimeric PC analogs was increased significantly when compared to natural dimeric PCs. This implies that the other bioactivities of the PC analogs might be enhanced as well, such as anthelmintic activity, and the results encourage to further study the PC analogs. The octanol–water partition and stability in PBS solution revealed additional information about the properties of the PC analogs. The results showed surprising variability in these properties despite the small structural differences between the tested compounds.

One major hypothesis leading to this thesis was that oligomeric and polymeric PA–Mv adducts could be detected using group-specific UPLC–MS/MS methodology. The method development was correspondingly one of the major successes in the experimental work of this thesis. Overall, 15 groups of anthocyanins and monomeric adducts of anthocyanins could be detected simultaneously in a single analysis, which corresponded to 45 or more individual compounds in a typical red wine sample. Importantly, three different groups of PA–Mv adducts could be separately detected with the developed method without being limited by the structure or degree of oligomerization of the PA moieties, or by the glycosidic units attached to the malvidin aglycones. This was the true novelty of the developed method. The produced 2D chromatographic fingerprints revealed that the oligomeric and polymeric adducts in red wine are indeed highly complex mixtures, and these mixtures have never been detected this comprehensively and with this much structural precision.

Plenty of screening studies of red wines have been conducted in the past but a new screening study into commercial red wines was well justified because of the

developed novel method. Therefore, over 300 commercial red wines were analyzed with the method to answer various research questions concerning basic properties of the oligomeric adducts, e.g., how their composition differs between wine types, how the adducts evolve in red wine, and how they contribute to color intensity of red wine. Especially the 2D chromatographic fingerprints, and the associated new visualization method of the chromatographic data, enabled conclusions that would have been impossible to make with other currently existing methods. These included, for instance, the subtle evolution in qualitative composition of the PA–Mv^+ and PA–Mv–FL adducts.

The adaption of the group-specific UPLC–MS/MS method might not be too time consuming for other researchers, should they only have access to a suitable MS system with tandem capabilities. Note, that the MS system does not necessarily have to be a triple quadrupole system to adopt the concept of the developed method. The quantification marker ions and the MRM transitions can be adopted as such, which only leaves the need for optimization of the instrument-dependent parameters to achieve efficient formation and detection of the quantification marker ions. The optimization of these parameters could be possible by just analyzing raw commercial red wines with no need to analyze fractions or isolated model compounds. The optimization of CEs (or other similar parameter) for further fragmentation of the quantification markers is important to maximize sensitivity. However, any parameters of the utilized instrument that related to the accumulation of the quantification markers do not need to be optimized with absolute accuracy because there are not some correct values that absolutely must be used. It is primarily important to produce several fingerprints of the detected oligomeric adducts that emphasize adducts with different degrees of oligomerization and sizes in different proportions. One good criterion for this process is presented in Article I: one fingerprint should emphasize the dimeric adducts, one trimeric oligomeric adducts and slightly higher oligomers, and one fingerprints should emphasize the highest oligomeric adducts that can be detected with the utilized instrument.

The purpose of the previous section was to encourage any chemist who is reading this, and is working with red wine, to go and try to adapt the UPLC–MS/MS method in their own laboratory. The author is confident that group-specific methodology could help in solving more red wine related research questions in the future as well. Moreover, this thesis focuses only on three different groups of oligomeric adducts, and the group-specific methodology could still be applied to many other groups of oligomeric adducts in red wine. Perhaps, in some time, the polyphenolic complexity of the unique oligomeric adducts in red wine can be resolved one chromatographic fingerprint at a time.

Acknowledgements

This doctoral research was carried out in the Natural Chemistry Research Group at the Department of Chemistry, University of Turku between 2018 and 2023. The Doctoral Programme in Physical and Chemical Sciences (now Doctoral Programme in Exact Sciences) of the University of Turku Graduate School is sincerely acknowledged for their continuous funding between January 2018 and May 2021, which enabled me to fully focus on the research. Turku University Foundation is acknowledged for supporting me with a grant during the finalization stages of the PhD project in 2023.

I am humbled by the encouraging comments of the pre-examiners of my thesis, Dr. Véronique Cheynier and Dr. Michael Jourdes. I hold your evaluations and comments in very high regard, and I thank you for agreeing to review my thesis. I wish to thank Dr. Nuno Mateus for agreeing to review my thesis and for agreeing to be my opponent in the dissertation defence.

Professor Juha-Pekka Salminen, the director and supervisor of my thesis, deserves my deepest gratitude for enabling this thesis. I want to take this opportunity to extend my gratitude beyond the thesis. When I was still an undecided second-year student trying to figure out what career path to pursue, you introduced me to a whole new world that I had no idea existed, the world of natural compound chemistry. Something sparked in me during those years, and the passion towards chemistry of nature has never left. Thank you for setting me on this path. Thank you Dr. Petri Tähtinen and Dr. Maarit Karonen for supervising my PhD thesis. You two have also been part of my entire journey at NCRG, and I wish to thank you for that as well, and not only for the supervision of my thesis. Your expertise and know-how have played a major role in making me the capable chemist that I am today.

I want to thank Jussi Suvanto, Dr. Jorma Kim, Suvi Vanhakylä, Dr. Marianna Manninen, Dr. Marica Engström, Dr. Valtteri Virtanen, Dr. Iqbal Bin Imran, Anne Koivuniemi, Mimosa Sillanpää, Ilari Kuukkanen, Niko Luntamo and Ville Fock for the enjoyable and often hilarious everyday life at NCRG. I got to share many great experiences with you, and some of those memories I will carry on with me for a long time and with a big smile on my face. Additionally, I wish to thank all former members of NCRG, and especially Dr. Nicolas Baert, Dr. Anu Tuominen, Dr.

Johanna Moilanen and Dr. Matti Vihakas. I looked up to you when I joined NCRG, your articles were the first scientific articles I ever read, and you were an inspiration to me. Thank you, Mauri Nauma, Kari Loikas and Kirsi Laaksonen for keeping the department running on daily basis and making the lives of the researchers, myself included, that much easier. A big thank you to everyone else at the Department of Chemistry as well.

I ended up taking a break from the PhD project between May 2021 and December 2022 when I worked as a customs chemist at the Custom Laboratory in Otaniemi, Espoo. This period might have been a complete break from the PhD work, but it was an invaluable period for my professional growth. More importantly, I wish to thank the wonderful people in the Customs Lab and in the Product Safety Unit for making me feel so welcomed and appreciated. I thoroughly enjoyed my time with you all.

Thank you, my dear friends, Sini Aaltonen, Sampo Hirvioja, Dr. Antti Äärelä, Eveliina Äärelä and Valtteri Jänkälä for your friendship and support in life.

I want to thank my parents Kari Laitila and Kaisa Mursu for their continuous and endless support in whatever I do. Your support is truly as unconditional as can be. I want to thank my sisters Jenna Laitila and Jutta Laitila for their support as well, and for being the best sisters a proud older brother could ever hope to have.

Topias, I had to work on this thesis almost throughout my paternity leave. Knowing that would happen, I was so worried beforehand that I would not be able to enjoy our time together to the fullest due to my mind being on the thesis, or due to being tired after late nights of working. Luckily, my worries were mostly for nothing. I had so much fun with you on our adventures in Espoo and Helsinki, we met great people at the library of Lippulaiva and at other places, and even the thesis was still completed. Thank you for being the delightful, cheeky, and happy little boy that you are.

Milla, it is not an exaggeration to say that this thesis would not have been completed by now without you. I needed your support more and more towards the end of this project, and you were there for me when I needed you. The feelings of joy and gratefulness are almost overwhelming every time I think about how incredibly lucky I am to have you, and Topias, in my life. Thank you.

Espoo, November 2023

List of References

Alberts, P., Stander, M. A., & De Villiers, A. (2012). Advanced ultra high pressure liquid chromatography–tandem mass spectrometric methods for the screening of red wine anthocyanins and derived pigments. *Journal of Chromatography A*, *1235*, 92–102. https://doi.org/10.1016/j.chroma.2012.02.058

Alcalde-Eon, C., Escribano-Bailón, M. T., Santos Buelga, C., & Rivas-Gonzalo, J. C. (2006). Changes in the detailed pigment composition of red wine during maturity and ageing: A comprehensive study. *Analytica Chimica Acta*, *563*(1–2), 238–254. https://doi.org/10.1016/j.aca.2005.11.028

Arapitsas, P., Perenzoni, D., Nicolini, G., & Mattivi, F. (2012). Study of Sangiovese Wines Pigment Profile by UHPLC-MS/MS. *Journal of Agricultural and Food Chemistry*, *60*(42), 10461–10471. https://doi.org/10.1021/jf302617e

Arapitsas, P., Ugliano, M., Marangon, M., Piombino, P., Rolle, L., Gerbi, V., Versari, A., & Mattivi, F. (2020). Use of Untargeted Liquid Chromatography-Mass Spectrometry Metabolome to Discriminate Italian Monovarietal Red Wines, Produced in Their Different Terroirs. *Journal of Agricultural and Food Chemistry*, *68*(47), 13353–13366. https://doi.org/10.1021/acs.jafc.0c00879

Araújo, P., Fernandes, A., Freitas, V., & Oliveira, J. (2017). A New Chemical Pathway Yielding A-type Vitisins in Red Wines. *International Journal of Molecular Sciences*, *18*(4), 762. https://doi.org/10.3390/ijms18040762

Baert, N. (2017). *Oligomeric Ellagitannins of Epilobium angustigolium: Quantification and Bioactivity assessment*. University of Turku.

Bakker, J., Bridle, P., Honda, T., Kuwano, H., Saito, N., Terahara, N., & Timberlake, C. F. (1997). Identification of an Anthocyanin Occurring in Some Red Wines. *Phytochemistry*, *44*(7), 1375–1382. https://doi.org/10.1016/S0031-9422(96)00707-8

Bakker, J., & Timberlake, C. F. (1985). The Distribution of Anthocyanins in Grape Skin Extracts of Port Wine Cultivars as Determined by High Performance Liquid Chromatography. *Journal of the Science of Food and Agriculture*, *36*(12), 1315–1324. https://doi.org/10.1002/jsfa.2740361217

Bakker, J., & Timberlake, C. F. (1997). Isolation, Identification, and Characterization of New Color-Stable Anthocyanins Occurring in Some Red Wines. *Journal of Agricultural and Food Chemistry*, *45*, 35–43. https://doi.org/10.1021/jf960252c

Baldi, A., Romani, A., Mulinacci, N., Vincieri, F. F., & Casetta, B. (1995). HPLC/MS Application to Anthocyanins of *Vitis vinifera* L. *Journal of Agricultural and Food Chemistry*, *43*, 2104–2109.

Bindon, K. A., Kassara, S., Hayasaka, Y., Schulkin, A., & Smith, P. A. (2014). Properties of Wine Polymeric Pigments Formed From Anthocyanin and Tannins Differing in Size Distribution and Subunit Composition. *Journal of Agricultural and Food Chemistry*, *62*(47), 11582–11593. https://doi.org/10.1021/jf503922h

Blanco-Vega, D., Gómez-Alonso, S., & Hermosín-Gutiérrez, I. (2014). Identification, content and distribution of anthocyanins and low molecular weight anthocyanin-derived pigments in Spanish commercial red wines. *Food Chemistry*, *158*, 449–458. https://doi.org/10.1016/j.foodchem.2014.02.154

Bloemberg, T. G., Gerretzen, J., Wouters, H. J. P., Gloerich, J., van Dael, M., Wessels, H. J. C. T., van den Heuvel, L. P., Eilers, P. H. C., Buydens, L. M. C., & Wehrens, R. (2010). Improved parametric

time warping for proteomics. *Chemometrics and Intelligent Laboratory Systems*, *104*(1), 65–74. https://doi.org/10.1016/j.chemolab.2010.04.008

Boido, E., Alcalde-Eon, C., Carrau, F., Dellacassa, E., & Rivas-Gonzalo, J. C. (2006). Aging Effect on the Pigment Composition and Color of *Vitis vinifera* L. Cv. Tannat Wines. Contribution of the Main Pigment Families to Wine Color. *Journal of Agricultural and Food Chemistry*, *54*(18), 6692–6704. https://doi.org/10.1021/jf061240m

Brouillard, R., & Delaporte, B. (1977). Chemistry of Anthocyanin Pigments. 2. Kinetic and Thermodynamic Study of Proton Transfer, Hydration, and Tautomeric Reactions of Malvidin 3-Glucoside. *Journal of the American Chemical Society*, *99*(26), 8461–8468. https://doi.org/0.1021/ja00468a015

Brouillard, R., & Dubois, J.-E. (1977). Mechanism of the Structural Transformations of Anthocyanins in Acidic Media. *Journal of the American Chemical Society*, *99*(5), 1359–1364. https://doi.org/10.1021/ja00447a012

Cala, O., Pinaud, N., Simon, C., Fouquet, E., Laguerre, M., Dufourc, E. J., & Pianet, I. (2010). NMR and molecular modeling of wine tannins binding to saliva proteins: Revisiting astringency from molecular and colloidal prospects. *FASEB Journal*, *24*(11), 4281–4290. https://doi.org/10.1096/fj.10-158741

Cameira-dos-Santos, P.-J., Brillouet, J.-M., Cheynier, V., & Moutounet, M. (1996). Detection and Partial Characterisation of New Anthocyanin-Derived Pigments in Wine. *Journal of the Science of Food and Agriculture*, *70*(2), 204–208. https://doi.org/10.1002/(SICI)1097-0010(199602)70:2<204::AID-JSFA484>3.0.CO;2-Fopen_in_new ISSN00

Cao, H., Högger, P., Arroo, R., & Xiao, J. (2020). Flavonols with a catechol or pyrogallol substitution pattern on ring B readily form stable dimers in phosphate buffered saline at four degrees celsius. *Food Chemistry*, *311*. https://doi.org/10.1016/j.foodchem.2019.125902

Castillo-Muñoz, N., Gómez-Alonso, S., García-Romero, E., & Hermosín-Gutiérrez, I. (2007). Flavonol Profiles of *Vitis vinifera* Red Grapes and Their Single-Cultivar Wines. *Journal of Agricultural and Food Chemistry*, *55*(3), 992–1002. https://doi.org/10.1021/jf062800k

Chatonnet, P., Dubourdieu, D., Boidron, J., & Lavigne, V. (1993). Synthesis of volatile phenols by Saccharomyces cerevisiae in wines. *Journal of the Science of Food and Agriculture*, *62*(2), 191–202. https://doi.org/10.1002/jsfa.2740620213

Chira, K., Jourdes, M., & Teissédre, P.-L. (2012). Cabernet sauvignon red wine astringency quality control by tannin characterization and polymerization during storage. *European Food Research and Technology*, *234*(2), 253–261. https://doi.org/10.1007/s00217-011-1627-1

Chira, K., Zeng, L., Le Floch, A., Péchamat, L., Jourdes, M., & Teissédre, P.-L. (2015). Compositional and sensory characterization of grape proanthocyanidins and oak wood ellagitannin. *Tetrahedron*, *71*(20), 2999–3006. https://doi.org/10.1016/j.tet.2015.02.018

Chung, J. E., Kurisawa, M., Kim, Y. J., Uyama, H., & Kobayashi, S. (2004). Amplification of Antioxidant Activity of Catechin by Polycondensation with Acetaldehyde. In *Biomacromolecules* (Vol. 5, Issue 1, pp. 113–118). https://doi.org/10.1021/bm0342436

Cruz, L., Petrov, V., Teixeira, N., Mateus, N., Pina, F. S., & Freitas, V. (2010). Establishment of the Chemical Equilibria of Different Types of Pyranoanthocyanins in Aqueous Solutions: Evidence for the Formation of Aggregation in Pyranomalvidin-3-*O*-coumaroylglucoside-(+)-catechin. *Journal of Physical Chemistry B*, *114*(41), 13232–13240. https://doi.org/10.1021/jp1045673

Dallas, C., Ricardo-da-Silva, J. M., & Laureano, O. (1996). Products Formed in Model Wine Solutions Involving Anthocyanins, Procyanidin B2, and Acetaldehyde. *Journal of Agricultural and Food Chemistry*, *44*(8), 2402–2407. https://doi.org/10.1021/jf940433j

Dangles, O., & Fenger, J. A. (2018). The chemical reactivity of anthocyanins and its consequences in food science and nutrition. *Molecules*, *23*, 1970. https://doi.org/10.3390/molecules23081970

Dimitrovska, M., Bocevska, M., Dimitrovski, D., & Murkovic, M. (2011). Anthocyanin composition of Vranec, Cabernet Sauvignon, Merlot and Pinot Noir grapes as indicator of their varietal

differentiation. *European Food Research and Technology*, *232*(4), 591–600. https://doi.org/10.1007/s00217-011-1425-9

Drinkine, J., Glories, Y., & Saucier, C. (2005). (+)-Catechin–Aldehyde Condensations: Competition Between Acetaldehyde and Glyoxylic Acid. *Journal of Agricultural and Food Chemistry*, *53*(19), 7552–7558. https://doi.org/10.1021/jf0504723

Drinkine, J., Lopes, P., Kennedy, J. A., Teissédre, P.-L., & Saucier, C. (2007a). Analysis of Ethylidene-Bridged Flavan-3-ols in Wine. *Journal of Agricultural and Food Chemistry*, *55*(4), 1109–1116. https://doi.org/10.1021/jf0626258

Drinkine, J., Lopes, P., Kennedy, J. A., Teissédre, P.-L., & Saucier, C. (2007b). Ethylidene-Bridged Flavan-3-ols in Red Wine and Correlation with Wine Age. *Journal of Agricultural and Food Chemistry*, *55*(15), 6292–6299. https://doi.org/10.1021/jf070038w

Dueñas, M., Salas, E., Cheynier, V., Dangles, O., & Fulcrand, H. (2006). UV−Visible Spectroscopic Investigation of the 8,8-Methylmethine Catechin-malvidin 3-Glucoside Pigments in Aqueous Solution: Structural Transformations and Molecular Complexation with Chlorogenic Acid. *Journal of Agricultural and Food Chemistry*, *54*(1), 189–196. https://doi.org/10.1021/jf0516989

Eilers, P. H. C. (2004). Parametric Time Warping. *Analytical Chemistry*, *76*(2), 404–411. https://doi.org/10.1021/ac034800e

Engström, M. T., Arvola, J., Nenonen, S., Virtanen, V. T. J., Leppä, M. M., Tähtinen, P., & Salminen, J. P. (2019). Structural Features of Hydrolyzable Tannins Determine Their Ability to Form Insoluble Complexes with Bovine Serum Albumin. *Journal of Agricultural and Food Chemistry*, *67*(24), 6798–6808. https://doi.org/10.1021/acs.jafc.9b02188

Engström, M. T., Karonen, M., Ahern, J. R., Baert, N., Payré, B., Hoste, H., & Salminen, J. P. (2016). Chemical Structures of Plant Hydrolyzable Tannins Reveal Their in Vitro Activity against Egg Hatching and Motility of Haemonchus contortus Nematodes. *Journal of Agricultural and Food Chemistry*, *64*(4), 840–851. https://doi.org/10.1021/acs.jafc.5b05691

Engström, M. T., Pälijärvi, M., Fryganas, C., Grabber, J. H., Mueller-Harvey, I., & Salminen, J.-P. (2014). Rapid Qualitative and Quantitative Analyses of Proanthocyanidin Oligomers and Polymers by UPLC-MS/MS. *Journal of Agricultural and Food Chemistry*, *62*(15), 3390–3399. https://doi.org/10.1021/jf500745y

Engström, M. T., Pälijärvi, M., & Salminen, J.-P. (2015). Rapid Fingerprint Analysis of Plant Extracts for Ellagitannins, Gallic Acid, and Quinic Acid Derivatives and Quercetin-, Kaempferol- and Myricetin-Based Flavonol Glycosides by UPLC-QqQ-MS/MS. *Journal of Agricultural and Food Chemistry*, *63*(16), 4068–4079. https://doi.org/10.1021/acs.jafc.5b00595

Engström, M. T., Virtanen, V., & Salminen, J. P. (2022). Influence of the Hydrolyzable Tannin Structure on the Characteristics of Insoluble Hydrolyzable Tannin-Protein Complexes. *Journal of Agricultural and Food Chemistry*, *70*(41), 13036–13048. https://doi.org/10.1021/acs.jafc.2c01765

Escribano-Bailón, M. T., Dangles, O., & Brouillard, R. (1996). Coupling reactions between flavylium ions and catechin. *Phytochemistry*, *41*(6), 1583–1592. https://doi.org/10.1016/0031-9422(95)00811-X

Escribano-Bailón, M. T., Rivas-Gonzalo, J. C., & García-Estévez, I. (2019). Wine Color Evolution and Stability. In *Red Wine Technology* (pp. 195–205). Academic Press. https://doi.org/10.1016/b978-0-12-814399-5.00013-x

Es-Safi, N.-E., Cheynier, V., & Moutounet, M. (2000). Study of the Reactions Between (+)-Catechin and Furfural Derivatives in the Presence or Absence of Anthocyanins and Their Implication in Food Color Change. *Journal of Agricultural and Food Chemistry*, *48*(12), 5946–5954. https://doi.org/10.1021/jf000394d

Es-Safi, N.-E., Cheynier, V., & Moutounet, M. (2002). Role of Aldehydic Derivatives in the Condensation of Phenolic Compounds with Emphasis on the Sensorial Properties of Fruit-Derived Foods. *Journal of Agricultural and Food Chemistry*, *50*(20), 5571–5585. https://doi.org/10.1021/jf025503y

Es-Safi, N.-E., Fulcrand, H., Cheynier, V., & Moutounet, M. (1999). Competition between (+)-Catechin and (–)-Epicatechin in Acetaldehyde-Induced Polymerization of Flavanols. *Journal of Agricultural and Food Chemistry*, *47*(5), 2088–2095. https://doi.org/10.1021/jf980628h

Es-Safi, N.-E., Le Guernevé, C., Fulcrand, H., Cheynier, V., & Moutounet, M. (2000). Xanthylium salts formation involved in wine colour changes. *International Journal of Food Science & Technology*, *35*(1), 63–74. https://doi.org/10.1046/j.1365-2621.2000.00339.x

Es-Safi, N.-E., Le Guernevé, C., Labarbe, B., & Fulcrand, H. (1999). Structure of a New Xanthylium Salt Derivative. *Tetrahedron Letters*, *40*, 5869–5872.

Fanzone, M., Zamora, F., Jofré, V., Assof, M., Gómez-Cordovés, C., & Peña-Neira, Á. (2012). Phenolic characterisation of red wines from different grape varieties cultivated in Mendoza province (Argentina). *Journal of the Science of Food and Agriculture*, *92*(3), 704–718. https://doi.org/10.1002/jsfa.4638

Freitas, V., & Mateus, N. (2002). Nephelometric study of salivary protein–tannin aggregates. *Journal of the Science of Food and Agriculture*, *82*(1), 113–119. https://doi.org/10.1002/jsfa.1016

Freitas, V., & Mateus, N. (2011). Formation of pyranoanthocyanins in red wines: A new and diverse class of anthocyanin derivatives. *Analytical and Bioanalytical Chemistry*, *401*(5), 1467–1477. https://doi.org/10.1007/s00216-010-4479-9

Friedrich, W., Eberhardt, A., & Galensa, R. (2000). Investigation of proanthocyanidins by HPLC with electrospray ionization mass spectrometry. *European Food Research and Technology*, *211*(1), 56–64. https://doi.org/10.1007/s002170050589

Fulcrand, H., Benabdeljalil, C., Rigaud, J., Cheynier, V., & Moutounet, M. (1998). A New Class of Wine Pigments Generated by Reaction Between Pyruvic Acid and Grape Anthocyanins. *Phytochemistry*, *47*(7), 1401–1407. https://doi.org/10.1016/S0031-9422(97)00772-3

Fulcrand, H., Cameira-dos-Santos, P. J., Sarni-Manchado, P., Cheynier, V., & Favre-Bonvin, J. (1996). Structure of new anthocyanin-derived pigments. *Journal of Chemical Society, Perkin Transactions I*, 735–739. https://doi.org/10.1039/P19960000735

Fulcrand, H., Cheynier, V., Oszmianski, J., & Moutounet, M. (1997). An Oxidized Tartaric Acid Residue as a New Bridge Potentially Competing with Acetaldehyde in Flavan-3-ol Condensation. *Phytochemistry*, *46*, 223–227.

García-Estévez, I., Escribano-Bailón, M. T., Rivas-Gonzalo, J. C., & Alcalde-Eon, C. (2012). Validation of a Mass Spectrometry Method to Quantify Oak Wllagitannins in Wine Samples. *Journal of Agricultural and Food Chemistry*, *60*(6), 1373–1379. https://doi.org/10.1021/jf203836a

García-Estévez, I., Ramos-Pineda, A. M., & Escribano-Bailón, M. T. (2018). Interactions between wine phenolic compounds and human saliva in astringency perception. *Food and Function*, *9*(3), 1294–1309. https://doi.org/10.1039/c7fo02030a

Gawel, R., Francis, L., & Waters, E. J. (2007). Statistical Correlations etween the In-Mouth Textural Characteristics and the Chemical Composition of Shiraz Wines. *Journal of Agricultural and Food Chemistry*, *55*(7), 2683–2687. https://doi.org/10.1021/jf0633950

Gilbert, M. (2016). Plastics Materials: Introduction and Historical Development. In *Brydson's Plastics Materials: Eighth Edition* (pp. 2–18). Elsevier Inc. https://doi.org/10.1016/B978-0-323-35824-8.00001-3

Gómez-Plaza, E., Olmos, O., & Bautista-Ortín, A. B. (2016). Tannin profile of different Monastrell wines and its relation to projected market prices. *Food Chemistry*, *204*, 506–512. https://doi.org/10.1016/j.foodchem.2016.02.124

Gris, E. F., Mattivi, F., Ferreira, A. E., Vrhovsek, U., Pedrosa, C. R., & Bordignon-Luiz, M. T. (2011). Proanthocyanidin profile and antioxidant capacity of Brazilian *Vitis vinifera* red wines. *Food Chemistry*, *126*(1), 213–220. https://doi.org/10.1016/j.foodchem.2010.10.102

Gross, J. H. (2017a). Hyphenated Methods. In *Mass Spectrometry - A Textbook* (Third Edit, pp. 831–887). Springer International Puglishing AG. https://doi.org/10.1007/978-3-319-54398-7

Gross, J. H. (2017b). Tandem Mass Spectrometry. In *Mass Spectrometry – A Textbook* (Third Edition, pp. 539–612). Springer.

Guo, A., Kontoudakis, N., Scollary, G. R., & Clark, A. C. (2017). Production and Isomeric Distribution of Xanthylium Cation Pigments and Their Precursors in Wine-like Conditions: Impact of Cu(II), Fe(II), Fe(III), Mn(II), Zn(II), and Al(III). *Journal of Agricultural and Food Chemistry*, *65*(11), 2414–2425. https://doi.org/10.1021/acs.jafc.6b05554

Guyot, S., Marnet, N., Laraba, D., Sanoner, P., & Drilleau, J.-F. (1998). Reversed-Phase HPLC following Thiolysis for Quantitative Estimation and Characterization of the Four Main Classes of Phenolic Compounds in Different Tissue Zones of a French Cider Apple Variety (*Malus domestica* Var. Kermerrien). *8561*(97), 1698–1705.

Hanlin, R. L., Kelm, M. A., Wilkinson, K. L., & Downey, M. O. (2011). Detailed Characterization of Proanthocyanidins in Skin, Seeds, and Wine of Shiraz and Cabernet Sauvignon Wine Grapes (*Vitis vinifera*). *Journal of Agricultural and Food Chemistry*, *59*(24), 13265–13276. https://doi.org/10.1021/jf203466u

Harbertson, J. F., Picciotto, E. A., & Adams, D. O. (2003). Measurement of Polymeric Pigments in Grape Berry Extracts and Wines Using a Protein Precipitation Assay Combined with Bisulfite Bleaching. *American Journal of Enology and Viticulture*, *54*(4), 301–306.

Haslam, E. (1980). *In vino veritas*: Oligomeric Procyanidins and the Ageing of Red Wines. *Phytochemistry*, *19*(12), 2577–2582. https://doi.org/10.1016/S0031-9422(00)83922-9

Hatano, T., Hori, M., Kusuda, M., Ohyabu, T., Ito, H., & Yoshida, T. (2004). Characaterization of the Oxidation Products of (–)-Epigallocatechin Gallate, a Bioactive Tea Polyphenols, on Incubation in Neutral Solution. *Heterocycles*, *63*(7), 1547–1554.

Hatano, T., Kusuda, M., Hori, M., Shiota, S., Tsuchiya, T., & Yoshida, T. (2003). Theasinensin A - a Tea Polyphenol Formed From (–)-Epigallocatechin Gallate, Suppresses Antibiotic Resistance of Methicillin-Resistant *Staphylococcus aureus*. *Planta Medica*, *69*, 984–989.

Hayasaka, Y., & Asenstorfer, R. E. (2002). Screening for Potential Pigments Derived from Anthocyanins in Red Wine Using Nanoelectrospray Tandem Mass Spectrometry. *Journal of Agricultural and Food Chemistry*, *50*(4), 756–761.

Hayasaka, Y., & Kennedy, J. A. (2003). Mass spectrometric evidence for the formation of pigmented polymers in red wine. *Australian Journal Of Grape And Wine Research*, *9*(3), 210–220. https://doi.org/10.1111/j.1755-0238.2003.tb00272.x

He, F., Liang, N. N., Mu, L., Pan, Q. H., Wang, J., Reeves, M. J., & Duan, C. Q. (2012). Anthocyanins and Their Variation in Red Wines II. Anthocyanin Derived Pigments and Their Color Evolution. In *Molecules* (Vol. 17, Issue 2, pp. 1483–1519). https://doi.org/10.3390/molecules17021483

He, J., Carvalho, A. R. F., Mateus, N., & Freitas, V. (2010). Spectral Features and Stability of Oligomeric Pyranoanthocyanin-Flavanol Pigments Isolated from Red Wines. *Journal of Agricultural and Food Chemistry*, *58*(16), 9249–9258. https://doi.org/10.1021/jf102085e

He, J., Oliveira, J., Silva, A. M. S., Mateus, N., & Freitas, V. (2010). Oxovitisins: A New Class of Neutral Pyranone-Anthocyanin Derivatives in Red Wines. *Journal of Agricultural and Food Chemistry*, *58*(15), 8814–8819. https://doi.org/10.1021/jf101408q

He, J., Santos Buelga, C., Mateus, N., & Freitas, V. (2006). Isolation and quantification of oligomeric pyranoanthocyanin-flavanol pigments from red wines by combination of column chromatographic techniques. *Journal of Chromatography A*, *1134*(1–2), 215–225. https://doi.org/10.1016/j.chroma.2006.09.011

Heath, R. (2017). Aldehyde Polymers: Phenolics and Aminoplastics. In *Brydson's Plastics Materials: Eighth Edition* (pp. 705–742). Elsevier Inc. https://doi.org/10.1016/B978-0-323-35824-8.00025-6

Jurd, L. (1969). Review of polyphenol condensation reactions and their possible occurance in the aging wine. *American Journal of Enology and Viticulture*, *20*, 191–195.

Kebarle, P. (2000). A brief overview of the present status of the mechanisms involved in electrospray mass spectrometry. *Journal of Mass Spectrometry*, *35*(7), 804–817. https://doi.org/10.1002/1096-9888(200007)35:7<804::AID-JMS22>3.0.CO;2-Q

Kennedy, J. A., & Jones, G. P. (2001). Analysis of Proanthocyanidin Cleavage Products Following Acid-Catalysis in the Presence of Excess Phloroglucinol. *Journal of Agricultural and Food Chemistry*, *49*(4), 1740–1746. https://doi.org/10.1021/jf001030o

Kim, Y. J., Uyama, H., & Kobayashi, S. (2004). Inhibition effects of (+)-catechin–aldehyde polycondensates on proteinases causing proteolytic degradation of extracellular matrix.

Biochemical and Biophysical Research Communications, *320*(1), 256–261. https://doi.org/10.1016/j.bbrc.2004.05.163

Lee, D. F., Swinny, E. E., & Jones, G. P. (2004). NMR identification of ethyl-linked anthocyanin–flavanol pigments formed in model wine ferments. *Tetrahedron Letters*, *45*(8), 1671–1674. https://doi.org/10.1016/j.tetlet.2003.12.110

Leppä, M. M., Laitila, J. E., & Salminen, J.-P. (2020). Distribution of Protein Precipitation Capacity within Variable Proanthocyanidin Fingerprints. *Molecules*, *25*(21), 5002. https://doi.org/10.3390/molecules25215002

Li, H. J., & Deinzer, M. L. (2007). Tandem Mass Spectrometry for Sequencing Proanthocyanidins. *Analytical Chemistry*, *79*(4), 1739–1748. https://doi.org/10.1021/ac061823v

Lopez, R., Aznar, M., Cacho, J., & Ferreira, V. (2002). Determination of minor and trace volatile compounds in wine by solid-phase extraction and gas chromatography with mass spectrometric detection. *Journal of Chromatography A*, *966*(1–2), 167–177. https://doi.org/10.1016/S0021-9673(02)00696-9

Lukić, I., Radeka, S., Budić-Leto, I., Bubola, M., & Vrhovsek, U. (2019). Targeted UPLC-QqQ-MS/MS profiling of phenolic compounds for differentiation of monovarietal wines and corroboration of particular varietal typicity concepts. *Food Chemistry*, *300*, 125251. https://doi.org/10.1016/j.foodchem.2019.125251

Mateus, N., Oliveira, J., Pissarra, J., González-Paramás, A. M., Rivas-Gonzalo, J. C., Santos Buelga, C., Silva, A. M. S., & Freitas, V. (2006). A new vinylpyranoanthocyanin pigment occurring in aged red wine. *Food Chemistry*, *97*(4), 689–695. https://doi.org/10.1016/j.foodchem.2005.05.051

Mazza, G. (1995). Anthocyanins in Grapes and Grape Products. *Critical Reviews in Food Science and Nutrition*, *35*(4), 341–371. https://doi.org/10.1080/10408399509527704

Mcrae, J. M., & Kennedy, J. A. (2011). Wine and Grape Tannin Interactions with Salivary Proteins and Their Impact on Astringency: A Review of Current Research. *Molecules*, *16*, 2348–2364. https://doi.org/10.3390/molecules16042348

Moss, R., Mao, Q., Taylor, D., & Saucier, C. (2013). Investigation of monomeric and oligomeric wine stilbenoids in red wines by ultra-high-performance liquid chromatography/electrospray ionization quadrupole time-of-flight mass spectrometry. *Rapid Communications in Mass Spectrometry*, *27*(16), 1815–1827. https://doi.org/10.1002/rcm.6636

Mueller-Harvey, I., Bee, G., Dohme-Meier, F., Hoste, H., Karonen, M., Kölliker, R., Lüscher, A., Niderkorn, V., Pellikaan, W. F., Salminen, J. P., Skøt, L., Smith, L. M. J., Thamsborg, S. M., Totterdell, P., Wilkinson, I., Williams, A. R., Azuhnwi, B. N., Baert, N., Brinkhaus, A. G., … Waghorn, G. C. (2019). Benefits of Condensed Tannins in Forage Legumes Fed to Ruminants: Importance of Structure, Concentration, and Diet Composition. *Crop Science*, *59*(3), 861–885. https://doi.org/10.2135/cropsci2017.06.0369

Nave, F., Petrov, V., Pina, F., Teixeira, N., Mateus, N., & Freitas, V. (2010). Thermodynamic and Kinetic Properties of a Red Wine Pigment: Catechin-(4,8)-Malvidin-3-*O*-Glucoside. *Journal of Physical Chemistry B*, *114*(42), 13487–13496. https://doi.org/10.1021/jp104749f

Nonier Bourden, M. F., Vivas, N., Absalon, C., Vitry, C., Fouquet, E., & Vivas de Gaulejac, N. (2008). Structural diversity of nucleophilic adducts from flavanols and oak wood aldehydes. *Food Chemistry*, *107*(4), 1494–1505. https://doi.org/10.1016/j.foodchem.2007.10.012

Oliveira, J., Freitas, V., Silva, A. M. S., & Mateus, N. (2007). Reaction between Hydroxycinnamic Acids and Anthocyanin–Pyruvic Acid Adducts Yielding New Portisins. *Journal of Agricultural and Food Chemistry*, *55*(15), 6349–6356. https://doi.org/10.1021/jf070968f

Oliveira, J., Mateus, N., & Freitas, V. (2013). Network of carboxypyranomalvidin-3-*O*-glucoside (vitisin A) equilibrium forms in aqueous solution. *Tetrahedron Letters*, *54*(37), 5106–5110. https://doi.org/10.1016/j.tetlet.2013.07.046

Pati, S., Losito, I., Gambacorta, G., La Notte, E., Palmisano, F., & Zambonin, P. G. (2006). Simultaneous separation and identification of oligomeric procyanidins and anthocyanin-derived

pigments in raw red wine by HPLC-UV-ESI-MSn. *Journal of Mass Spectrometry*, *41*(7), 861–871. https://doi.org/10.1002/jms.1044

Peng, Z., Iland, P. G., Oberholster, A., Sefton, M. A., & Waters, E. J. (2002). Analysis of pigmented polymers in red wine by reverse phase HPLC. *Australian Journal of Grape and Wine Research*, *8*(1), 70–75. https://doi.org/10.1111/j.1755-0238.2002.tb00213.x

Pina, F. S., Oliveira, J., & Freitas, V. (2015). Anthocyanins and derivatives are more than flavylium cations. *Tetrahedron*, *71*(20), 3107–3114. https://doi.org/10.1016/j.tet.2014.09.051

Pissarra, J., Lourenço, S., González-Paramás, A. M., Mateus, N., Santos Buelga, C., Silva, A. M. S., & Freitas, V. (2005). Isolation and structural characterization of new anthocyanin-alkyl-catechin pigments. *Food Chemistry*, *90*(1–2), 81–87. https://doi.org/10.1016/j.foodchem.2004.03.027

Pissarra, J., Mateus, N., Rivas-Gonzalo, J. C., Santos Buelga, C., & Freitas, V. (2003). Reaction Between Malvidin 3-Glucoside and (+)-Catechin in Model Solutions Containing Different Aldehydes. *Journal of Food Science*, *68*(2), 476–481. https://doi.org/10.1111/j.1365-2621.2003.tb05697.x

Quideau, S., Deffieux, D., Douat-Casassus, C., & Pouységu, L. (2011). Plant Polyphenols: Chemical Properties, Biological Activities, and Synthesis. *Angewandte Chemie International Edition*, *50*(3), 586–621. https://doi.org/10.1002/anie.201000044

Quijada-Morín, N., Dangles, O., Rivas-Gonzalo, J. C., & Escribano-Bailón, M. T. (2010). Physico-Chemical and Chromatic Characterization of Malvidin 3-Glucoside-Vinylcatechol and Malvidin 3-Glucoside-Vinylguaiacol Wine Pigments. *Journal of Agricultural and Food Chemistry*, *58*(17), 9744–9752. https://doi.org/10.1021/jf102238v

Quijada-Morín, N., Regueiro, J., Simal-Gándara, J., Tomás, E., Rivas-Gonzalo, J. C., & Escribano-Bailón, M. T. (2012). Relationship between the Sensory-Determined Astringency and the Flavanolic Composition of Red Wines. *Journal of Agricultural and Food Chemistry*, *60*(50), 12355–12361. https://doi.org/10.1021/jf3044346

R core team. (2022). *R: A language and environment for statistical computing* (4.2.2). R Foundation for Statistical Computing.

Remy, S., Fulcrand, H., Labarbe, B., Cheynier, V., & Moutounet, M. (2000). First confirmation in red wine of products resulting from direct anthocyanin–tannin reactions. *Journal of the Science of Food and Agriculture*, *80*(6), 745–751. https://doi.org/10.1002/(SICI)1097-0010(20000501)80:6<745::AID-JSFA611>3.0.CO;2-4

Remy-Tanneau, S., Le Guernevé, C., Meudec, E., & Cheynier, V. (2003). Characterization of a Colorless Anthocyanin–Flavan-3-ol Dimer Containing Both Carbon-Carbon and Ether Interflavanoid Linkages by NMR and Mass Spectrometry. *Journal of Agricultural and Food Chemistry*, *51*(12), 3592–3597. https://doi.org/10.1021/jf021227b

Ristic, R., Bindon, K., Francis, L. I., Herderich, M. J., & Iland, P. G. (2010). Flavonoids and C_{13}-norisoprenoids in *Vitis vinifera* L. cv. Shiraz: Relationships between grape and wine composition, wine colour and wine sensory properties. *Australian Journal of Grape and Wine Research*, *16*(3), 369–388. https://doi.org/10.1111/j.1755-0238.2010.00099.x

Ritz, C., Baty, F., Streibig, J. C., & Gerhard, D. (2015). Dose-Response Analysis Using R. *PLOS ONE*, *10*(12), e0146021. https://doi.org/10.1371/journal.pone.0146021

Rohart, F., Gautier, B., Singh, A., & Cao, K.-A. (2017). mixOmics: An R package for 'omics feature selection and multiple data integration. *PLOS Computational Biology*, *13*(11), e1005752. https://doi.org/10.1371/journal.pcbi.1005752

Ropiak, H. M., Lachmann, P., Ramsay, A., Green, R. J., & Mueller-Harvey, I. (2017). Identification of Structural Features of Condensed Tannins That Affect Protein Aggregation. *PLOS ONE*, *12*(1), e0170768. https://doi.org/10.1371/journal.pone.0170768

Rstudio team. (2022). *RStudio: Integrated Development Environment for R* (2022.12.0.353). http://www.rstudio.com/

Salas, E., Atanasova, V., Poncet-Legrand, C., Meudec, E., Mazauric, J. P., & Cheynier, V. (2004). Demonstration of the occurrence of flavanol-anthocyanin adducts in wine and in model solutions. *Analytica Chimica Acta*, *513*(1), 325–332. https://doi.org/10.1016/j.aca.2003.11.084

Salas, E., Fulcrand, H., Meudec, E., & Cheynier, V. (2003). Reactions of Anthocyanins and Tannins in Model Solutions. *Journal of Agricultural and Food Chemistry*, *51*(27), 7951–7961. https://doi.org/10.1021/jf0345402

Salminen, J.-P. (2018). Two-Dimensional Tannin Fingerprints by Liquid Chromatography Tandem Mass Spectrometry Offer a New Dimension to Plant Tannin Analyses and Help to Visualize the Tannin Diversity in Plants. *Journal of Agricultural and Food Chemistry*, *66*(35), 9162–9171. https://doi.org/10.1021/acs.jafc.8b02115

Salminen, J.-P., & Karonen, M. (2011). Chemical ecology of tannins and other phenolics: We need a change in approach. *Functional Ecology*, *25*(2), 325–338. https://doi.org/10.1111/j.1365-2435.2010.01826.x

Sanchez, G. (2012). *plsdepot: Partial Least Squares (PLS) Data Analysis Methods* (R package version 0.1.17). https://cran.r-project.org/package=plsdepot

Sánchez-Ilárduya, M. B., Sánchez-Fernández, C., Garmón-Lobato, S., Abad-García, B., Berrueta, L. À., Gallo, B., & Vicente, F. (2014). Detection of non-coloured anthocyanin-flavanol derivatives in Rioja aged red wines by liquid chromatography-mass spectrometry. *Talanta*, *121*, 81–88. https://doi.org/10.1016/j.talanta.2013.12.066

Saucier, C., Little, D., & Glories, Y. (1997). First Evidence of Acetaldehyde-Flavanol Condensation Products in Red Wine. *American Journal of Enology and Viticulture*, *48*(3), 370–373.

Schwarz, M., Wabnitz, T. C., & Winterhalter, P. (2003). Pathway Leading to the Formation of Anthocyanin–Vinylphenol Adducts and Related Pigments in Red Wines. *Journal of Agricultural and Food Chemistry*, *51*(12), 3682–3687. https://doi.org/10.1021/jf0340963

Sheridan, M. K., & Elias, R. J. (2015). Exogenous acetaldehyde as a tool for modulating wine color and astringency during fermentation. *Food Chemistry*, *177*, 17–22. https://doi.org/10.1016/j.foodchem.2014.12.077

Shoji, T., Goda, Y., Toyoda, M., Yanagida, A., & Kanda, T. (2002). Characterization and structures of anthocyanin pigments generated in rosé cider during vinification. *Phytochemistry*, *59*(2), 183–189. https://doi.org/10.1016/S0031-9422(01)00427-7

Soares, S., García-Estévez, I., Ferrer-Galego, R., Brás, N. F., Brandão, E., Silva, M., Teixeira, N., Fonseca, F., Sousa, S. F., Ferreira-da-Silva, F., Mateus, N., & Freitas, V. (2018). Study of human salivary proline-rich proteins interaction with food tannins. *Food Chemistry*, *243*(February 2017), 175–185. https://doi.org/10.1016/j.foodchem.2017.09.063

Somers, T. C. (1971). The polymeric nature of wine pigments. *Phytochemistry*, *10*(9), 2175–2186. https://doi.org/10.1016/S0031-9422(00)97215-7

Sun, W., & Miller, J. M. (2003). Tandem mass spectrometry of the B-type procyanidins in wine and B-type dehydrodicatechins in an autoxidation mixture of (+)-catechin and (–)-epicatechin. *Journal of Mass Spectrometry*, *38*(4), 438–446. https://doi.org/10.1002/jms.456

Swain, T., & Hillis, W. E. (1959). The phenolic constituents of *Prunus domestica* I. – The quantitative analysis of phenolic constituents. *Journal of the Science of Food and Agriculture*, *10*, 63–68.

Tanaka, T., Mine, C., Watarumi, S., Fujioka, T., Mihashi, K., Zhang, Y. J., & Kouno, I. (2002). Accumulation of Epigallocatechin Quinone Dimers During Tea Fermentation and Formation of Theasinensins. *Journal of Natural Products*, *65*(11), 1582–1587. https://doi.org/10.1021/np020245k

Teng, B., Hayasaka, Y., Smith, P. A., & Bindon, K. A. (2019). Effect of Grape Seed and Skin Tannin Molecular Mass and Composition on the Rate of Reaction with Anthocyanin and Subsequent Formation of Polymeric Pigments in the Presence of Acetaldehyde. *Journal of Agricultural and Food Chemistry*, *67*(32), 8938–8949. https://doi.org/10.1021/acs.jafc.9b01498

Timberlake, C. F., & Bridle, P. (1976). Interactions between Anthocyanins, Phenolic Compounds, and Acetaldehyde and Their Significange in Red Wines. *American Journal of Enology and Viticulture*, *27*(3), 97–106.

Vallverdú-Queralt, A., Meudec, E., Eder, M., Lamuela-Raventos, R. M., Sommerer, N., & Cheynier, V. (2017). The Hidden Face of Wine Polyphenol Polymerization Highlighted by High-Resolution Mass Spectrometry. *ChemistryOpen*, *6*(3), 336–339. https://doi.org/10.1002/open.201700044

Vera, M., & Urbano, B. F. (2021). Tannin polymerization: An overview. *Polymer Chemistry*, *12*(30), 4272–4290. https://doi.org/10.1039/d1py00542a

Vidal, S., Francis, L., Noble, A., Kwiatkowski, M., Cheynier, V., & Waters, E. (2004). Taste and mouth-feel properties of different types of tannin-like polyphenolic compounds and anthocyanins in wine. *Analytica Chimica Acta*, *513*(1), 57–65. https://doi.org/10.1016/j.aca.2003.10.017

Virtanen, V., & Karonen, M. (2020). Partition Coefficients (*logP*) of Hydrolysable Tannins. *Molecules*, *25*(16). https://doi.org/10.3390/molecules25163691

Vivar-Quintana, A. M., Santos Buelga, C., Francia-Aricha, E., & Rivas-Gonzalo, J. C. (1999). Formation of anthocyanin-derived pigments in experimental red wines. *Food Science and Technology International*, *5*(4), 347–352. https://doi.org/10.1177/108201329900500407

Wang, L., Du, G., Liu, P., Wang, X., Zhao, P., Zhang, Q., Lei, X., Yuan, H., Chen, T., & Wang, X. (2022). Characterization of wine astringency contributed by acetaldehyde-mediated condensation between flavan-3-ols and grape skin/seeds polyphenol. *Food Science and Technology*, *42*, e85022. https://doi.org/10.1590/FST.85022

Watrelot, A. A., Byrnes, N. K., Heymann, H., & Kennedy, J. A. (2016). Understanding the Relationship between Red Wine Matrix, Tannin Activity, and Sensory Properties. *Journal of Agricultural and Food Chemistry*, *64*(47), 9116–9123. https://doi.org/10.1021/acs.jafc.6b03767

Wickham, H. (2016). *ggplot2: Elegant Graphics for Data Analysis*. Springer-Verlag New York. https://ggplot2.tidyverse.org

Willemse, C. M., Stander, M. A., Vestner, J., Tredoux, A. G. J., & De Villiers, A. (2015). Comprehensive Two-Dimensional Hydrophilic Interaction Chromatography (HILIC) × Reversed-Phase Liquid Chromatography Coupled to High-Resolution Mass Spectrometry (RP-LC-UV-MS) Analysis of Anthocyanins and Derived Pigments in Red Wine. *Analytical Chemistry*, *87*(24), 12006–12015. https://doi.org/10.1021/acs.analchem.5b03615

Xu, J., Tan, T., Kenne, L., & Sandström, C. (2009). The use of diffusion-ordered spectroscopy and complexation agents to analyze mixtures of catechins. *New Journal of Chemistry*, *33*(5), 1057–1063. https://doi.org/10.1039/b900164f

Zeller, W. E., Sullivan, M. L., Mueller-Harvey, I., Grabber, J. H., Ramsay, A., Drake, C., & Brown, R. H. (2015). Protein Precipitation Behavior of Condensed Tannins from *Lotus pedunculatus* and *Trifolium repens* with Different Mean Degrees of Polymerization. *Journal of Agricultural and Food Chemistry*, *63*(4), 1160–1168. https://doi.org/10.1021/jf504715p

Zeng, L., Teissédre, P.-L., & Jourdes, M. (2016). Structures of polymeric pigments in red wine and their derived quantification markers revealed by high-resolution quadrupole time-of-flight mass spectrometry. *Rapid Communications in Mass Spectrometry*, *30*(1), 81–88. https://doi.org/10.1002/rcm.7416

Zhang, X. K., Lan, Y. Bin, Huang, Y., Zhao, X., & Duan, C. Q. (2021). Targeted metabolomics of anthocyanin derivatives during prolonged wine aging: Evolution, color contribution and aging prediction. *Food Chemistry*, *339*, 127795. https://doi.org/10.1016/j.foodchem.2020.127795

TURUN
YLIOPISTO
UNIVERSITY
OF TURKU

ISBN 978-951-29-9531-8 (PRINT)
ISBN 978-951-29-9532-5 (PDF)
ISSN 0082-7002 (Print)
ISSN 2343-3175 (Online)

Painosalama Oy, Turku, Finland 2023